Deep Learning-Aided Data Detection for Future Wireless Communication Systems

Thesis · January 2020

1 author:

Merve Gülmez
KU Leuven
9 PUBLICATIONS **21** CITATIONS

SEE PROFILE

ISTANBUL TECHNICAL UNIVERSITY ★ GRADUATE SCHOOL OF SCIENCE, ENGINEERING AND TECHNOLOGY

DEEP LEARNING AIDED DATA DETECTION FOR FUTURE WIRELESS COMMUNICATION SYSTEMS

M.Sc. THESIS

Merve TURHAN

Electronics and Communications Engineering Department

Telecommunications Engineering Programme

DECEMBER 2019

ISTANBUL TECHNICAL UNIVERSITY ★ GRADUATE SCHOOL OF SCIENCE, ENGINEERING AND TECHNOLOGY

DEEP LEARNING AIDED DATA DETECTION FOR FUTURE WIRELESS COMMUNICATION SYSTEMS

M.Sc. THESIS

Merve TURHAN
(504161354)

Electronics and Communications Engineering Department

Telecommunications Engineering Programme

Thesis Advisor: Prof. Dr. Hakan Ali ÇIRPAN

DECEMBER 2019

İSTANBUL TEKNİK ÜNİVERSİTESİ ★ FEN BİLİMLERİ ENSTİTÜSÜ

GELECEK NESİL TELSİZ HABERLEŞME SİSTEMLERİ İÇİN DERİN ÖĞRENME YARDIMIYLA DATA TESPİTİ

YÜKSEK LİSANS TEZİ

Merve TURHAN
(504161354)

Elektronik ve Haberleşme Mühendisliği Anabilim Dalı

Telekomünikasyon Mühendisliği Programı

Tez Danışmanı: Prof. Dr. Hakan Ali ÇIRPAN

ARALIK 2019

Merve TURHAN, a M.Sc. student of ITU Graduate School of Science, Engineering and Technology 504161354 , successfully defended the thesis entitled "DEEP LEARNING AIDED DATA DETECTION FOR FUTURE WIRELESS COMMUNICATION SYSTEMS", which she prepared after fulfilling the requirements specified in the associated legislations, before the jury whose signatures are below.

Thesis Advisor :	**Prof. Dr. Hakan Ali ÇIRPAN** Istanbul Technical University	.....
Jury Members :	**Assoc. Prof. Ender Mete EKŞİOĞLU** Istanbul Technical University	.....
	Dr. Ersin ÖZTÜRK NETAŞ	.....

Date of Submission : **15 November 2019**
Date of Defense : **12 December 2019**

To my family,

FOREWORD

The work presented in this thesis was conducted during my M.Sc study at Telecommunication Engineering Program of Electronics and Communication Engineering Department at Istanbul Technical University Graduate School of Science Engineering and Technology. I would like to take this opportunity to acknowledge all the people who have supported me.

First of all, I would like to express my gratitude to Prof. Dr. Hakan Ali ÇIRPAN, he is my supervisor and gave me a chance to be a graduate student. Then, I also want to express my gratitude to Dr. Ersin ÖZTÜRK for steering me into this interesting research topic and for continuous support throughout this research work. I greatly appreciate his excellent guidance, trust, and support during my master's degree process. I also thank Prof. Andreas Burg and the Telecommunications Circuit Laboratory for providing me with new experiences. I also would like to thank TUBITAK for funding support. Furthermore, I would like to thank NETAŞ for their everlasting support. Lastly, I want to express my gratitude to my family and my friends.

The studies conducted in this thesis have been published two international conference papers. Also, one international journal paper has been submitted.

Hope that, this thesis would be helpful to researchers about deep learning-aided for future wireless networks.

December 2019 Merve TURHAN

TABLE OF CONTENTS

Page

ABBREVIATIONS

3GPP	**:** Third Generation Partnership Project
5G	**:** Fifth Generation
Adam	**:** Adaptive Moment Estimation
AWGN	**:** Additive White Gaussion Noise Channel
BPSK	**:** Binary Phase Shift Keying
BER	**:** Bit Error Ratio
CIR	**:** Channel Impulse Response
CM	**:** Complex Multiplication
CNN	**:** Convolutional Neural Network
CP	**:** Cyclic Prefix
DNN	**:** Deep Neural Network
EPA	**:** Extended Pedestrian A
FCNN	**:** Fully Connected Neural Network
GFDM	**:** Generalized Frequency Division Multiplexing
GPU	**:** Graphics Processing Units
IM	**:** Index Modulation
JDD	**:** Joint Detection and Demodulation
ML	**:** Maximum Likelihood
MMSE	**:** Minimum Mean-Squared Error
MIMO	**:** Multiple-Input Multiple-Output
PHY	**:** Physical Layer
QAM	**:** Quadrature Amplitude Modulation
OFDM	**:** Orthogonal Frequency Division Multiplexing
OOB	**:** Out-of-Band
RC	**:** Raised Cosine
SNR	**:** Signal-to-Noise Ratio
SISO	**:** Single-Input Single-Output
SM	**:** Spatial Modulation
SMX	**:** Spatial Multiplexing
ZF	**:** Zero-Forcing

SYMBOLS

$(\cdot)^{\mathbf{T}}$	: Transposition of a vector or a matrix
$(\cdot)^{\mathbf{H}}$	: Hermitian transposition of a vector or a matrix
$(\cdot)^{-1}$	: Inverse of a matrix
$(\cdot)^{+}$	: Pseudo-inverse of a matrix
$C(u,v)$	: The binomial coefficient
$\lfloor \cdot \rfloor$	: The floor function
$\Re\{X\}$	: The real part of a complex variable X
$\Im\{X\}$	: The imaginary part of a complex variable X
$\|\cdot\|$	: The Euclidean norm
$\mathscr{S}$	: Q-ary signal constellation
$N_{\mathbf{CP}}$	: Length of cyclic prefix
$N_{\mathbf{Ch}}$	: Tap length of the communication channel
E_b	: The average transmitted energy per bit
E_s	: The average transmitted energy per symbol
N_0	: The noise power spectral density
$\mathscr{CN}(0,\sigma_X^2)$	: The distribution of a circularly symmetric complex Gaussian random variable $\mathbf{X}$ with variance σ_X^2

LIST OF TABLES

Page

LIST OF FIGURES

Page

DEEP LEARNING AIDED DATA DETECTION FOR FUTURE WIRELESS COMMUNICATION SYSTEMS

SUMMARY

The demand for reliable, fast and effective wireless communication methods go on with the growing trend thanks to new applications which have challenging technical requirements. In this sense, orthogonal frequency division multiplexing (OFDM) with multiple numerologies concept has been proposed to meet the requested key performance indicators of fifth generation (5G) wireless networks by Third Generation Partnership Project (3GPP). Although OFDM has solid advantages, e.g., simple equalization, robustness to frequency selective fading and easy implementation, the inabilities of OFDM such as high out-of-band (OOB) emission and high peak-to-average power ratio (PAPR), make it quite disputable to meet the expectations from the physical layer (PHY) of future wireless access technologies. Therefore, improved PHY techniques need to be developed for beyond 5G wireless networks. Generalized frequency division multiplexing (GFDM) is one of the notable attempts to cope with the challenges of future wireless networks. GFDM provides advantages in terms of latency, spectral efficiency, and OOB emission because of block-based structure, reduced overhead of cyclic prefix (CP) and subcarrier-based digital pulse shaping, respectively. The featured benefit of GFDM is the flexibility that enables time-frequency engineering according to the requirements of the target application. Index modulation (IM) techniques offer energy and spectral efficiency by utilizing transmission entities to convey digital information innovatively. Also, multiple-input multiple-output (MIMO) has an important ability for a PHY scheme to match the foreseen requirements beyond the 6G.

Deep learning has lately attracted important attention because of its high performance to solve computationally-burdened problems in various fields such as object detection, recommendation systems, and computer vision. Considering the unprecedented success of deep learning in various problems, researchers are eagerly attempting to exploit it for wireless communication.

In this thesis, GFDM, GFDM with IM and Spatial Multiplexing (SMX) with IM scheme has been examined and novel receiver schemes have been proposed in order to meet the next generation's physical layer requirements.

In the first stage of the thesis, general concepts about the data detection method for wireless networks and deep learning methods undertaking in this thesis are explained shortly.

In the second stage of the thesis, deep learning-aided joint detection and demodulation (JDD) scheme is proposed for GFDM scheme. Detection and demodulation of the GFDM blocks include coarse and fine detection stages, which are implemented by using a linear detector and a neural network in a cascaded manner. This application would be the first attempt to exploit a neural network for GFDM detection. Besides,

minimum mean-squared error (MMSE) detector is proposed for the coarse detection stage of the cascaded approach. Furthermore, a convolutional neural network (CNN) is exploited to handle complex signals, i.e., quadrature amplitude modulation (QAM) signals, through fully-connected neural network (FCNN). deep learning-aided JDD provides bit error ratio (BER) improvement compared to classical linear detectors.

In the third stage of the thesis, a novel deep convolutional neural network-based detector (DeepConvIM) is proposed for GFDM-IM scheme in order to reduce the complexity while improving error performance. The proposed detector first applies ZF detector to the received signal and then uses a neural network, which is composed of a CNN and an FCNN, to recover the transmitted information from the noisy channel outputs. This two-stage approach prevents the getting stuck of neural networks in a saddle point and enables IM blocks processing independently. Also, the FCNN part has only two fully-connected layers, which can be adapted to yield a trade-off between complexity and BER performance. Besides, the CNN has three important advantages that can help improve a deep learning model in terms of sparse interactions, parameter sharing, and equivalent representations. The proposed method would be the first attempt to exploit a neural network for GFDM-IM detection. Furthermore, a CNN approach is used to detect IM scheme for the first time. It has been demonstrated that the DeepConvIM provides essential BER improvement compared to ZF detector with a reasonable complexity increase.

In the fourth stage of the thesis, deep learning-aided data detection of SMX multiple-input multiple-output MIMO transmission with IM (Deep-SMX-IM) has been proposed in order to improve error performance without increasing complexity. Deep-SMX-IM has been constructed by combining ZF detector and DL technique. The main contribution of this proposed method is to use CNN and FCNN to learn the transmission characteristics of spatial and frequency multiplexing, respectively. Note that, a CNN approach provides a flexible structure for SMX transmission thanks to supporting the multi-channel operation and preserving the spatial dependence. Besides, using IM enables to implement subblock-based detection, which simplifies the DL model and reduces the complexity. The proposed method would be the first appearance to implement DL-aided SMX with IM (SMX-IM) detection. The Deep-SMX-IM provides important BER improvement compared to ZF detector without increasing complexity.

In this thesis, deep learning-aided JDD for GFDM, DeepConvIM for GFDM-IM and Deep-SMX-IM for SMX-IM have been proposed. All proposed models provide significant BER performance but while deep learning-aided JDD has the highest complexity, Deep-SMX-IM has the lowest complexity. The use of index modulation techniques in deep learning-aided detection methods ensures that deep learning-aided models are of low complexity. Furthermore, the combination of SMX and IM ensures that the complexity remains almost the same compared to the linear detector. It has been concluded that significant advantages of deep learning techniques should be engineered to overcome the challenges of wireless communications arising from the distinct characteristics of time, frequency and spatial domains.

GELECEK NESİL TELSİZ HABERLEŞME SİSTEMLERİ İÇİN DERİN ÖĞRENME YARDIMIYLA DATA TESPİTİ

ÖZET

Güvenilir hızlı ve efektif telsiz haberleşme yöntemleri teknik açıdan zorluklara sahip yeni uygulamalar ile gelişen bir alan olarak devam etmektedir. Bu çerçevede 5. nesil telsiz haberleşme ağlarının mevcut teknik zorluklarını karşılamak amaçlı çoklu parametre kümesine sahip dik frekans bölmeli çoğullama (orthogonal frequency division multiplexing, OFDM) istenen performansları karşılamak amacıyla önerilmiştir. Ancak telsiz haberleşme kullanıcıları ve uygulamaları sayılarında görülen artış eğilimi nedeniyle OFDM tabanlı bir fiziksel katmanın yeterliliği yeni nesil fiziksel katman teknikleri için tartışmalıdır. Bu nedenden dolayı 5. nesil sonrası haberleşme sistemleri için yeni telsiz haberleşme yöntemlerine ihtiyaç duyulduğu konusunda yaygın bir düşünce bulunmaktadır.

Genelleştirilmiş Frekans Bölmeli Çoğullama (Generalized Frequency Division Multiplexing, GFDM), son yıllarda öne çıkmış gelecek nesil haberleşme sistemlerinin zorluklarıyla başa çıkmak için ön görülen bir fiziksel katman tekniğidir. GFDM zaman frekans kaynağı planlamasına izin vermesiyle iletim gecikmesine karşı, düşürülmüş çevrimsel önek (cyclic prefix) ile uzaysal verimliliğe karşı, her alttaşıyıcının bir süzgeçten geçirilmesiyle OOB yayılıma karşı çözüm getirmektedir.

Indis Modülasyonu (index modulation, IM) modülasyonu spektrum ve uzaysal verimliliği nedeniyle oldukça ilgi görmüş basit bir sayısal modülasyon tekniğidir. Geleneksel sayısal modülasyonların tersine, IM iletişim sisteminin yapıtaşları olan anten, zaman dilimi gibi bilgilerin var olup olmamasını kullanarak bilgi iletimi yapar. Uzaysal modulasyon bilgi iletmek için antenleri kullanırken, OFDM-IM sistemlerde alt taşıyıcı pozisyonlarının var/yok mekanizmasıyla bilgi iletimi için kullanılır. Buna göre bazı alt taşıyıcılar kullanılmaz. Bu sayede kullanılmayan alt taşıyıcıların enerjileri, kullanılan alt taşıyıcılara aktarılarak bit başına düşen enerji miktarı artırılır ve bit hata oranı başarımında artış sağlanır.

Gün geçtikçe artan veri hızı ve kullanıcı sayısı, frekans spektrumundaki sınırlılık nedeniyle araştırmacıları spectral verimliği artırmak için çözüm yollarına yöneltmiştir. Çok girişli çok çıkışlı sistemler (multiple input multiple output, MIMO) buna çözüm olarak sunulan yenilikçi bir yaklaşımdır. MIMO sistemlerde alıcı ve verici tarafta eş zamanlı çoklu anten kümesini kullanarak iletim ve alım yapar. Herhangi bir band genişliği ve yüksek iletim gücü olmadan yüksek kanal kapasitesi ve yüksek hız oranı sunar. Yeni nesil fiziksel katman çözümleri için spektral verimliliğe sahip MIMO iletim teknikleri ile çalışabilmek bir gerekliliktir.

Kablosuz haberleşmede yaşanan tüm bu gelişmelerin yanında, çeşitli modulasyon tekniklerine ve dalga formlarına göre gönderilen verinin alıcı tarafta tespit edilmeside yeni nesil haberleşme sistemlerinde geliştirilmesi gerekli bir konu haline gelmiştir. En büyük olabilirlik yöntemi en optimum yöntemi sunsa da karmaşıklığı oldukça

yüksektir. Doğrusal tespit yöntemleri karmaşıklığı düşük sonuçlar sunar, ancak başarımı en büyük olabirlik yöntemine göre oldukça düşüktür. Bu kapsamda yeni nesil kablosuz haberleşme sistemlerinde alıcı dizaynında karmaşıklığı düşük başarımı yüksek alıcı modellerine ihtiyaç vardır.

Makine öğrenmesi bilgisayar biliminin hızla gelişen alanlarından biridir. En basit haliyle verilerden otomatik olarak pattern çıkarma işlemi olarak tanımlanır. Derin öğrenme ise makine öğrenmesinin alt alanlarından biridir. Son 10 yılda internet erişimin artmasıyla toplanan verilerin miktarı artmıştır. Bu daha fazla işlem gücü gerektiren bilgisayarlara ve öğrenme kapasitesi yüksek algoritmalara olan ihtiyacı artırmıştır. Bu kapsamda grafik işlem birimlerinin (graphical user interrface, GPU) hesaplamalarda kullanılması ve yeni algoritmaların geliştirilmesiyle derin öğrenme alanında oldukça ilerleme sağlanmış, nesne tespiti doğal dil işleme bilgisayarlı görü gibi alanlarda ciddi gelişmeler olmuştur. Derin sinir ağlarını (deep neural network, DNN) algoritmaların en başında tam bağlanmış sinir ağı (fully connected neural network, FCNN) gelmektedir. FCNN herhangi bir durum hafızası içermeyen girişten çıkışa kadar ileriye doğru yol içeren neural networklardır. FCNN yanında, resim gibi yerel değerlendirme istenilen uygulamalar için evrişimsel sinir ağı (convolutional neural network, CNN) geliştirilmiştir. CNN uzay boyunca ağırlıkları paylaşır, bu da FCNN göre daha az parametre ile işlem yapılmasını sağlar. Zamana bağlılığı olan veriler için ise durum hafıza bilgisi tutan yineleyen sinir ağı (recurrent neural network, RNN) geliştirilmiştir. RNN'ler ise zamansal boyutta ağırlıklarını paylaşır.

Tüm bu gelişmelerin yanında derin öğrenme telsiz haberleşme içinde ilgi çekici bir alan haline gelmiştir. Araştırmacıların ilgisini çekmiş, kanal tahmini, kanal kodlama, OFDM alıcılar ve MIMO tespiti ile ilgili çalışmalar yapılmıştır.

Bu tezde gelecek nesil fiziksel katman gereklilerini karşılamak amacıyla veri tespiti uygulamaları üzerine çalışılmıştır. Yeni nesil fiziksel katman çözümlerine önemli bir yer sahip ortogonal ve non-orthogonal dalga formalarının tespiti üzerine odaklanılmıştır. Spektral ve enerji verimliliği nedeniyle öne çıkan IM ve spectral verimliği sayesinde öne çıkan MIMO için data tespiti üzerine çalışılmıştır. Yeni alıcı tasarımı önerilmiştir.

Tezin ilk aşamasında geleneksel veri tespit yöntemlerinden olan en büyük olabilirlik yöntemi ve lineer tespit yöntemlerinden ve bu tezde uygulanan derin öğrenme destekli yapılacak kablosuz haberleşme çalışmasında kullanılan genel aşamalardan bahsedilmiştir. Bu aşamalar eğitim ve test datasının üretilmesi, derin öğrenme modelinin oluşturulması, eğitimin gerçekleşmesi ve test aşamasıdır.

Tezin ikinci aşamasında GFDM tespiti için derin öğrenme yardımıyla iki katmanlı alıcı yapısı önerilmiştir. Bu alıcı tarafı ana detektör ve yardımcı detektör kısımlarından oluşmaktadır. Ana tespit kısmında klasik tespit yöntemleri kullanılırken yardımcı tespit kısmında derin öğrenme kısmı kullanılmıştır. Derin öğrenme yardımıyla yapılan ilk GFDM uygulamasıdır. Derin öğrenme çerçevelerinin kompleks sayılar tarafından desteklenmemesi nedeniyle evrişimsel sinir ağı buna çözüm olarak sunulmuştur. Aynı zamanda ana tespit kısmında MMSE kullanılması derin öğrenme yardımıyla yapılan ilk uygulamalardandır. Bu uygulamanın sağladığı bit hata oranı (bit error rate, BER) başarımı iyi olsa da derin öğrenme kısmı oldukça kompleks bir katman yapısına sağlanmıştır.

Tezin üçüncü aşamasında GFDM-IM için bit hata oranını geliştirecek derin evrişimsel neural network bazlı tespit ve demodulation modeli önerilmiştir. Önerilen sistem ilk başta alınan sinyali sıfır zorlamalı detektörden geçirdikten sonra CNN ve ardından FCNN kullanan bir network modeli kullanır. Ana tespit kısmı yapıldıktan sonra IM bloklar birbirinden bağımsız bir şekilde derin öğrenme tarafından değerlendirilir. IM blokların birbirinden bağımsız değerlendirilmesi derin öğrenme kısmında basit bir model yapısı kullanmayı sağlar. GFDM-IM için tespit kısmı için derin öğrenme destekli ilk uygulamadır. Bu da yaptığımız modelin karmaşıklığını kabul edilebilir bir şekilde artırarak BER başarımı sağlar.

Tezin dördüncü aşamasında non-orthogonal ve orthogonal dalga formaları için SMX-IM data tespit kısmı için çalışılmıştır. Burada ana tespit yapıldıktan sonra IM blokları anten bazlı gruplandırılarak alt bloklara dönüştürülür. Her bir alt blok anten alt taşıyıcı konumları ve kompleks real boyutu olmak üzere 3 boyutta değerlendirilir. Her bir alt blok CNN algoritmasından yararlanılarak değerlendirilir. GFDM ve OFDM MIMO-IM alıcı tarafı için yapılan ilk ve yenilikçi bir algoritmadır. BER başarımında önemli bir gelişme sağlanırken modelin karmaşıklığı ZF ile hemen hemen aynıdır

Bu tezde GFDM, GFDM-IM ve SMX-IM için derin öğrenme destekli alıcı modeli önerilmiştir. Önerilen tüm methodlar bit hata oranı başarımını sağlamıştır. GFDM için karmaşık modelle öğrenim sağlanırken, GFDM-IM için kabul edilebilir bir karmaşıklıkla model önerilmiştir. SMX-IM için önerilen modelin karmaşıklığı doğrusal tespit yöntemleri ile karmaşıklığıyla hemen hemen aynı kalmıştır. Derin öğrenme yardımlı data tespiti metotlarının IM ve SMX-IM modelleri için gelecek kablosuz haberleşme sistemleri için önem arz edeceği ön görülmektedir.

1. INTRODUCTION

Wireless communication is a type of data communication that is performed and delivered without being connected to fixed locations. As wireless communication has become an essential part of daily activities, the demand for reliable, fast and effective wireless communication methods goes on with the growing trend. Besides, the burst of advanced wireless applications i.e. augmented reality, internet of things and virtual reality, has pushed the development of wireless communication in order to reach thousandfold capacity, millisecond latency, and massive connectivity.

Deep learning is one of the most rapidly developing and interesting fields of computer science in recent years. The goal of deep learning algorithms is to find an approximation of an unknown function. The main advantage of deep learning is high learning capacity and no need to feature extraction manually. Although the definition of deep learning was made in 1986, there has been no significant development until the last 10 years. Thanks to the development of GPU, neural network architecture and optimization algorithms, deep learning has a significant improvement to solve complex problems in miscellaneous fields, e.g. natural language processing, object detection, computer vision. Also, it has become an important area for communication systems, especially for physical layer problems.

In this sense, it is obvious that the demand for wireless communication continues to grow with new applications and deep learning application has a significant development for several areas. Therefore, deep learning aided wireless communication system comes to prominence for future wireless communication.

1.1 Literature Review

OFDM with multiple numerologies concept has been proposed to meet the requested key performance indicators of 5G wireless networks by 3GPP [1, 2]. Although OFDM has solid advantages, e.g., simple equalization, robustness to frequency selective fading and easy implementation, the inabilities of OFDM such as OOB emission and high

PAPR, make it quite disputable to meet the expectations from the PHY of future wireless access technologies [3]. Recently, several waveform proposals have been presented to overcome the above limitations of OFDM.

GFDM [4] is one of the prominent non-CP-OFDM-based waveforms to cope with the challenges of future wireless networks. GFDM provides advantages in terms of latency, spectral efficiency, and OOB emission because of block-based structure, reduced overhead of CP and subcarrier-based digitally pulse shaping, respectively. The featured benefit of GFDM is the flexibility that enables time-frequency engineering according to the requirements of the target application.

IM techniques [5] offer energy and spectral efficiency by utilizing transmission entities to convey digital information innovatively. While SM [6, 7] utilizes the transmit antennas of a MIMO transmission scheme, OFDM-IM [8–10] utilizes the subcarrier indices in a multi-carrier system to provide alternative ways for transmitting information. Taking account the efficiencies provided by IM, GFDM with IM has been considered and innovative transceiver schemes have been introduced [11–16]. In [11], the application of the SM-GFDM system has been considered. In [12], the combination of the IM technique with GFDM has been investigated. In [13], the combination of GFDM with SM and IM techniques has been considered. In [14], a GFDM-based flexible IM transceiver, which is capable of generating and decoding various IM schemes has been proposed. In [15], flexible IM numerology has been proposed to optimize OOB emission, spectral efficiency, and latency jointly. Furthermore, in [16], a novel MIMO-GFDM scheme, which combines SMX and MIMO transmission, GFDM and IM, has been proposed. Despite having optimized transceiver schemes in terms of OOB emission, spectral and energy efficiency, GFDM-IM schemes suffer high computational complexity with respect to conventional OFDM schemes.

Deep learning has recently attracted significant attention because of its high performance to solve computationally-burdened problems in various fields such as object detection, natural language processing, and computer vision [17]. Considering the unprecedented success of deep learning in classification problems, researchers are eagerly attempting to exploit it for wireless communication. In [18], a pair of blind detectors systems based on the clustering concept has been proposed for SM. In [19], a deep learning-based framework has been presented for channel estimation problem in

OFDM. In [20], a ZF detector followed by a deep neural network has been proposed for OFDM detection. In [21], a deep complex convolutional network has been developed as an OFDM receiver. In [22] and [23], a communication system has been considered as an autoencoder and communicating binary information through an impaired channel has been treated as reconstruction optimization over impairment layers in a channel autoencoder. This approach has been extended to multi-antenna case in [24]. In [25–27], deep learning-based MIMO detection schemes have been proposed. Besides, the use of deep learning has also been considered for uplink/downlink channel calibration in massive MIMO systems [28]. In [29] and [30], deep learning has been exploited for OFDM-IM and GFDM, respectively. Furthermore [31], deep learning aided SMX-IM has been examined. For a comprehensive overview of deep learning aided wireless communication, interested readers are referred to [32–35].

1.2 Original Contributions

In this thesis study, deep learning aided data detection schemes are proposed for GFDM, GFDM-IM, and SMX-IM.

In the first stage of the thesis, a deep neural network for GFDM symbol detection and demodulation is considered. The contributions of the first stage of the thesis can be summarized as follows:

- The main contribution is to propose a new architecture for the detection and demodulation of the GFDM blocks including coarse and fine detection stages, which are implemented by using a linear detector and a neural network in a cascaded manner. This model is termed as DL-aided JDD.
- Linear MMSE detector is proposed for the coarse detection stage of the cascaded approach.
- CNN is exploited to handle complex signals, i.e., QAM signals, through FCNN.
- Proposed scheme provides significant BER improvement compared to classical linear detectors with increasing complexity

In the second stage of the thesis, a deep neural network for GFDM-IM is considered. The contributions of the second stage of the thesis can be summarized as follows:

- The main contribution is to propose a novel deep convolutional neural network-based detector is proposed for GFDM-IM scheme. This model is termed as DeepConvIM.
- This two-stage approach prevents the getting stuck of neural networks in a saddle point and enables IM blocks processing independently.
- The FCNN part uses only two fully-connected layers, which can be adapted to yield a trade-off between complexity and BER performance
- CNN approach is used to detect IM scheme to improve a deep learning model in terms of sparse interactions, parameter sharing, and equivalent representations for the first time.
- The proposed scheme has a straightforward and flexible neural network structure, which can be adapted to yield a tradeoff between complexity and BER performance.

In the third stage of the thesis, a deep neural network for SMX-IM is considered. The contributions of the third stage of the thesis can be summarized as follows:

- A DNN-aided detector is proposed for the combined application of SMX MIMO transmission, GFDM, and IM for the purpose of improving error performance without increasing complexity. This model is termed as Deep-SMX-IM.
- The main contribution of this proposed model is to use a CNN to adapt the transmission characteristics of spatial multiplexing and to apply a FCNN to learn the transmitting properties of frequency multiplexing.
- Using IM enables to implement subblock-based detection simplifies the DL model and reduces the complexity
- A CNN approach provides a flexible structure for SMX transmission thanks to supporting multi-channel operation and preserves the spatial dependence
- The proposed method would be the first appearance to implement DL-aided SMX-IM detection
- It has been shown that the proposed method has an important BER gain competed with ZF detector with the same complexity

The sections in this thesis are organized as follows. In Section 2, general concepts about the subjects undertaking in this thesis are explained shortly. In Section 3, the deep learning aided GFDM detection is presented. Deep convolutional aided detector is proposed for GFDM-IM in Section 4. Deep Learning Aided Spatial Multiplexing with IM techniques are analyzed in Section 5. Section 6 presents the results of this thesis.

2. GENERAL CONCEPTS

In this section, the general concept of data detector and deep learning method are explained briefly.

2.1 General Concept of Data Detector

The wireless communication systems can be expressed as

$$\mathbf{y} = \mathbf{H}\mathbf{x} + \mathbf{w}. \tag{2.1}$$

where $\mathbf{y}$ represents the $R \times 1$ vector of received signals, $\mathbf{x}$ denotes T-dimensional transmitted symbol, $\mathbf{H}$ is the $R \times T$ channel matrix, $\mathbf{w}$ is an $R \times 1$ vector of AWGN samples with elements distributed as $\mathscr{CN}(0, \sigma_w^2)$.

For wireless communication systems detection of data from noisy measurements of transmitted signals is defined as a challenging problem. There are a lot of algorithms various trade-offs between performance and computational complexity.

2.1.1 Maximum likelihood

ML is the optimal detector in sense of minimizing the probability of error. This detector for the problem in equation 2.1 can be obtained as

$$\hat{\mathbf{x}} = \underset{\mathbf{x} \in \{\mathscr{X}\}}{\operatorname{argmin}} \|\mathbf{y} - \mathbf{H}\mathbf{x}\|^2, \tag{2.2}$$

Here, The ML computes overall probable transmitted vectors given the measurements y. It is obvious that ML detection suffers from the exponentially increasing computational complexity.

2.1.2 Linear detector

Linear Detector has low-complexity and simple but their solution is sub-optimal. These detectors are based linear transformation to the received symbols which then followed a minimum distance quantization. These methods try to decouple the effects of channel

spatially. There are two common methods for Linear Detector: These are ZF and MMSE detectors.

ZF technique is simplest detection technique and multiplies the received symbol vector by an equalization matrix. This matrix can be expressed as

$$\mathbf{G}_{\mathrm{ZF}} = \mathbf{H}^{+} = \left(\mathbf{H}^{\mathrm{H}}\mathbf{H}\right)^{-1}\mathbf{H}^{\mathrm{H}} \tag{2.3}$$

Here, it is assumed that $\mathbf{H}$ is invertible. At the decision step, each element of the filter output vector

$$\widehat{\mathbf{x}}_{\mathrm{ZF}} = \mathbf{G}_{\mathrm{ZF}}\mathbf{y} = \mathbf{x} + \left(\mathbf{H}^{\mathrm{H}}\mathbf{H}\right)^{-1}\mathbf{H}^{\mathrm{H}}\mathbf{w} \tag{2.4}$$

is mapped onto an element of the symbol constellation by a minimum distance quantization.

The performance of the ZF detection is reduced because of the $\left(\mathbf{H}^{\mathrm{H}}\mathbf{H}\right)^{-1}\mathbf{H}^{\mathrm{H}}\mathbf{w}$. To reduce for the this noise enhancement, the MMSE detector was proposed. The MMSE detection takes consider into the noise variance and reduces the noise enhancement by using the minimum mean square error. The estimation of the noise variance is very simple and it does not cause high complexity to the overall systems. MMSE detector uses

$$\mathbf{G}_{\mathrm{MMSE}} = \left(\mathbf{H}^{\mathrm{H}}\mathbf{H} + \sigma_w^2\mathbf{I}_T\right)^{-1}\mathbf{H}^{\mathrm{H}}, \tag{2.5}$$

where $\mathbf{I}_T$ is a $T \times T$ identity matrix. The resulting filter output is given by

$$\widehat{\mathbf{x}}_{\mathrm{MMSE}} = \mathbf{G}_{\mathrm{MMSE}}\mathbf{y} = \left(\mathbf{H}^{\mathrm{H}}\mathbf{H} + \sigma_w^2\mathbf{I}_T\right)^{-1}\mathbf{H}^{\mathrm{H}}\mathbf{y}. \tag{2.6}$$

The linear MMSE detector achieves better performance at low SNRs than the ZF detector thanks to noise enhancement.

2.2 General Concept of Deep Learning

The use of general concepts related to deep learning has been shown in Fig 2.1. There are four main stages in the general concept of deep learning, these are data generation, building model, training step and testing step.

2.2.1 Data generation

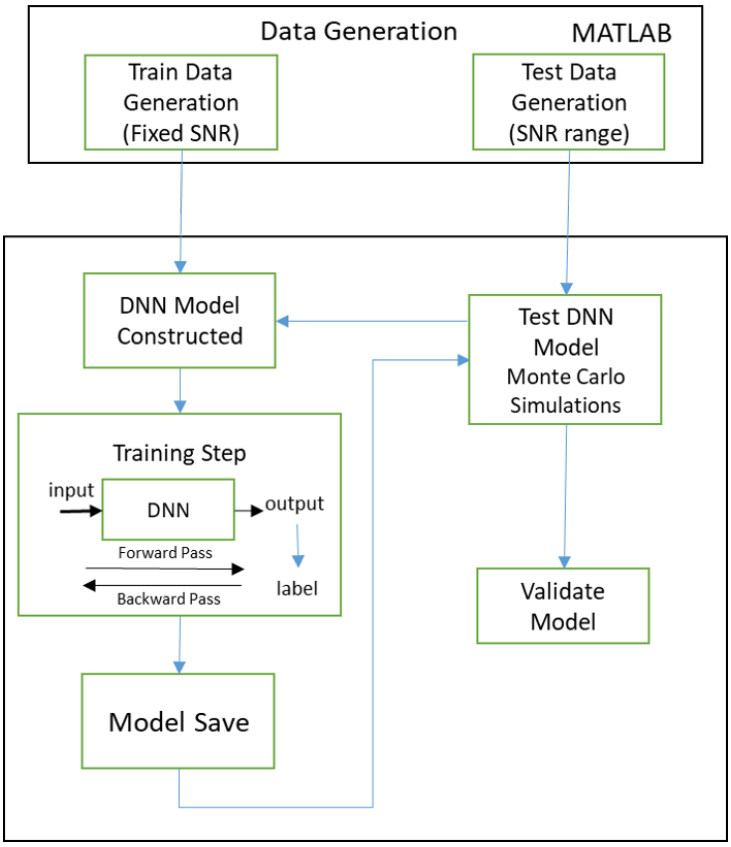

Figure 2.1 : The General Concept of Deep Learning aided Wireless Communication Application

Deep learning algorithms need to process large datasets in order to learn a pattern. The full exponential increase of wireless devices has led to the corresponding growth of traffic data [36]. This makes it easy to collect data for deep learning-aided next-generation communication systems. In this thesis, MATLAB simulation has been used for generating data. Training data has to be generated by fixed SNR. Training SNR value has a key role because low SNR can model to learn noise patterns and in contrary high SNR value can a cause solution that is not robust. The testing data has been generated for a range of SNR values.

2.2.2 Building model

The most important advantage of DL model is that it can solve a nonlinear problem that can not be solved by a linear expression thanks to its nonlinear activation functions. Activation functions also provide to normalize the output of each neuron. That is why activation functions, which are used in the last layer in deep learning aided detection

problems, are so essential. If symbol detection is required by a neural network or bit detection, it is necessary to use an activation function either $f_{tanh}(x) = \frac{e^x - e^{-x}}{e^x + e^{-x}}$, whose range is $(-1,1)$; or $f_{sigmoid}(x) = \frac{1}{1+e^{-x}}$, whose range is $(0,1)$, respectively. In this thesis, the used activation function can be seen in Fig. 2.4.

The simplest model of DNN is defined as a neuron, which is inspired by the neuron of the human brain, as seen in Fig. 2.3. Each neuron gets an input vector, multiplies them by their weights and applies activation functions. This process can be represented as:

$$h_1 = \phi(\mathbf{W}^T\mathbf{x} + b) \tag{2.7}$$

where h_1 represents output of each neuron, x is an input vector and W, b, ϕ denote weight matrix, bias term and activation functions, respectively .

A fully connected neural network, which consists of neurons, defines that each neuron in one layer is connected the all other neurons in the previous layer and next layer, but neurons within a single layer don't share any connections as seen in Fig 2.2. A FCNN describes as $f(x_0;\theta) : R^{N_0} \rightarrow R^{N_L}$ for $l = 1 \ldots L$, where x, L and θ are an input vector, number of layer and trainable parameters, respectively. Throughout the iterative process, a FCNN can be expressed as

$$x_l = f_l(x_{l-1};\theta_l) = \phi(\mathbf{W}_l^T\mathbf{x}_{l-1} + b_l) \tag{2.8}$$

for lth layer. Here, ϕ is an activation function and W_l, b_l are weights and bias term, respectively.

The convolution neural network is a specialized DL model and represents a vision of the human brain. It consists of convolution layer whose learning parameters are defined as kernel filter W^f, for $f = 1 \ldots F$. A convolution layer generally gets a multidimensional array. During the forward pass, each kernel filter has convolved a part of the input vector which has the same dimension, i.e. kernel filter has slid across an input vector according to stride size. In doing so, because the same kernel filter weights are used throughout the entire input data, the complexity decreases according to FCNN. The sum of the products of the corresponding elements is the output of the convolution layer. This process can be expressed as

$$Y_{i,j}^{f} = \sum_{k=0}^{a-1} \sum_{l=0}^{b-1} W_{a-k,b-l}^{f} X_{1+s(i-1)-k,1+s(j-1)-l} \tag{2.9}$$

where s is stride, W is $a \times b$ kernel filter, X denotes $\alpha \times \beta$ input matrix, Y represents $\alpha' = 1 + \frac{\alpha + a - 2}{s} \times \beta' = 1 + \frac{\beta + b - 2}{s}$ feature matrix. The convolution operator provide to reduce the input image to its important features. Besides, CNN has important advantages, these are sparse interactions, parameter sharing, equivalent representations [17].

The parameters used to set the model are hyperparameter and model parameters. While hyperparameter represents untrainable parameters such as layer size, a number of the neuron, learning rate, model parameters represent trainable parameters weight and bias. Hyperparameter, which needs to be set before the training process starts, the choice is a tricky and unknown step, because there is no strict rule or formula to choose right hyperparameters. It depends on searching and tuning operations over the deep learning model.

2.2.3 Training stage

Deep learning model consists of multiple layers, connections between these layers, a lot of parameters which are required to be tuned. The main goal of DL is to optimize model parameters in order to minimize loss functions. A loss function quantifies the difference between the estimated output of the model and the correct output. In this thesis, the mean squared error is used as a loss function. It can be explained as

$$loss_{MSE}(y, \hat{y}) = \frac{1}{n} \sum_{t=1}^{n} (y - \hat{y})^2 \tag{2.10}$$

where y and $\hat{y}$ represent expected output and calculated output respectively. The cost function calculates an average of loss function using a part of a training data set. According to this cost function, gradient descent-based optimization methods try to adjust model parameters iteratively. This optimization method calculates the local gradient of the cost function according to each model parameter, and its goal is to descend gradient until the algorithm converges to a minimum. This process can be expressed as

$$\theta_{+} = \theta - \eta \bigtriangledown loss(\theta), \tag{2.11}$$

where η represents learning rate, which describes as size of the gradient descents step, and θ refers to trainable parameters. In order to find global minimum, a lot of gradient descent algorithms have to be developed such as Adam [37], Adagrad, RMSProp and Momentum. In this thesis, the latest trend optimization Adam [37] is used as gradient descent methods.

The main purpose of the training model is not to learn the training data very well, but to give the same result in the test data. Therefore models are expected to find low generalization error as a result of training. Over-fitting is defined as the model has a high generalization error. Preventing overfitting has an important role during the training stage. Dropout scheme, adding regularization terms, early stopping are some methods for preventing overfitting.

Training deep learning models involves intensive matrix multiplications on an extremely dataset. This type of computing can be time-consuming. GPU, which has a large number of cores and specialized in running multiple computations simultaneously, can speed up the training process significantly. Models with high accuracy can be achieved in a short time with GPU.

In this thesis, three different DL model has been constructed for data detection. The first model, termed as DL-aided JDD, is built so complex. But DeepConvIM and Deep-SMX-IM have a very basic structure thanks to index modulation and spatial multiplexing. So, it is concluded that DeepConvIM and Deep-SMX-IM are more useful for future wireless networks thanks to index modulation.

2.2.4 Testing stage

After the training stage, model must be tested with the generated test data for each SNR value by using Monte Carlo simulation. If the training results do not give sufficient BER performance as reasonable increasing complexity, the hyper-parameters need to be changed and the model should be trained again.

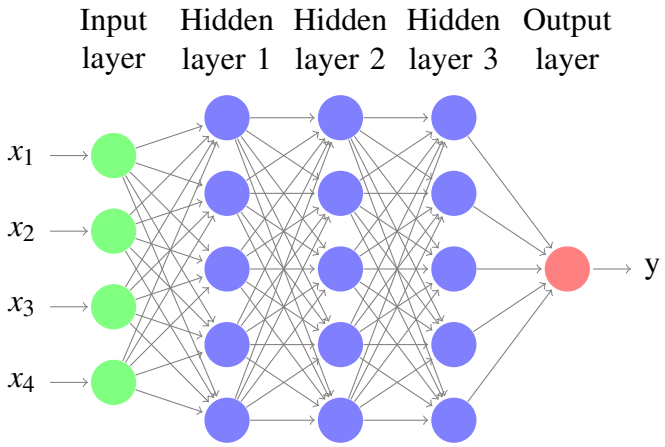

Figure 2.2 : Fully Connected Neural Network

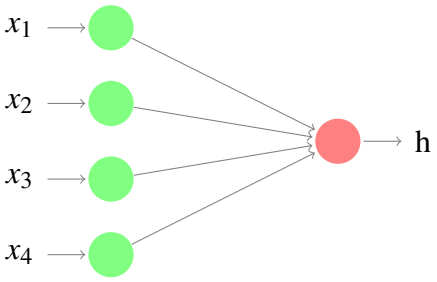

Figure 2.3 : The Most Simplest Model of Deep learning: Neuron

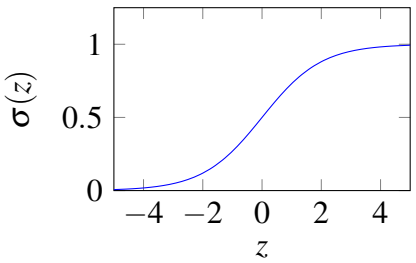

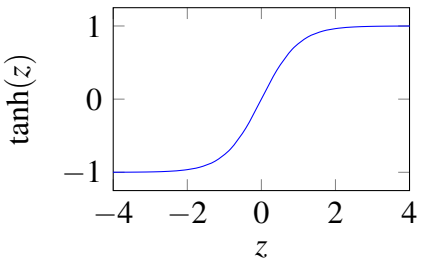

(b) Hyperbolic tangent activation function.

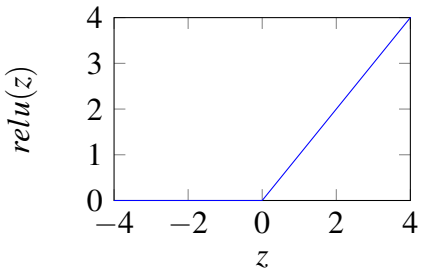

(c) Relu activation function.

Figure 2.4 : Common Used Activation Functions

3. GENERALIZED FREQUENCY DIVISION MULTIPLEXING

In this stage, GFDM scheme has been examined and deep learning aided JDD scheme has been proposed. In Section I, the system model for GFDM is presented. In Section II, deep learning aided GFDM detection and demodulation is presented. Numerical results are provided in Section III.

3.1 System Model for GFDM

A GFDM symbol $\mathbf{d} = [\mathbf{d}_0, \mathbf{d}_1, \ldots, \mathbf{d}_{M-1}]^{\mathrm{T}}$ has a block-based structure, which can be decomposed into M subsymbols, each consisting of K subcarriers, i.e., $\mathbf{d}_m = [d_{0,m}, d_{1,m}, \ldots, d_{K-1,m}]^{\mathrm{T}}$, for $m = 0, 1, \ldots, M-1$. Here, $d_{k,m}$ is the symbol from a 2^{γ}-valued complex constellation, where γ is the modulation order, transmitted on the k-th subcarrier of the m-th subsymbol of the GFDM symbol, $(\cdot)^{\mathrm{T}}$ shows the transposition of a vector. The total number of symbols in a GFDM symbol equals to $N = KM$. The block diagram of the GFDM transceiver is shown in Fig. 3.1. At the baseband processing stage of the GFDM transmit signal, each $d_{k,m}$ is cyclically-filtered by using a pulse shape

$$g_{k,m}(n) = g\left((n - mK)_{\mathrm{mod}N}\right) \exp\left(j2\pi \frac{kn}{K}\right), \tag{3.1}$$

where n denotes the sampling index. Here, $g_{k,m}(n)$ is a time and frequency shifted version of a prototype filter $g(n)$, where the modulo operation and the complex exponential perform the shifting operations in time and frequency, respectively. Then, the overall GFDM transmit signal is obtained by superposition of all transmit symbols

$$x(n) = \sum_{k=0}^{K-1} \sum_{m=0}^{M-1} d_{k,m} g_{k,m}(n). \tag{3.2}$$

After collecting the filter samples in a vector $\mathbf{g}_{k,m} = \left[g_{k,m}(0), \ldots, g_{k,m}(N-1)\right]^{\mathrm{T}}$, Eq. 3.2 can be rewritten as

$$\mathbf{x} = \mathbf{A}\mathbf{d}, \tag{3.3}$$

where $\mathbf{A}$ represents a $KM \times KM$ transmitter matrix [4] with the following structure:

$$\mathbf{A} = \left[\mathbf{g}_{0,0}, \ldots, \mathbf{g}_{K-1,0}, \mathbf{g}_{0,1}, \ldots, \mathbf{g}_{K-1,1}, \ldots, \mathbf{g}_{K-1,M-1}\right]. \tag{3.4}$$

As a last step of the GFDM baseband processing at the transmitter side, a CP with length N_{CP} is added to $\mathbf{x}$ to make the convolution with the channel circular. The resulting vector

$$\widetilde{\mathbf{x}} = \left[\mathbf{x}\left(KM - N_{\mathrm{CP}} + 1 : KM\right)^{\mathrm{T}}, \mathbf{x}^{\mathrm{T}}\right]^{\mathrm{T}}, \tag{3.5}$$

where $\mathbf{x}(a:b)$ shows all elements of $\mathbf{x}$ with indices from a to b, inclusive of a and b, is transmitted over a frequency-selective Rayleigh fading channel.

At the receiver side, assuming that perfect synchronization is ensured, CP is longer than the tap length of the channel (N_{Ch}) and the wireless channel stays constant during the transmission of a GFDM block, the received signal vector $\mathbf{y}$ can be obtained as

$$\mathbf{y} = \mathbf{H}\mathbf{x} + \mathbf{n} \tag{3.6}$$

after the removal of CP. Here, $\mathbf{y} = [y(0), y(1), \ldots, y(N-1)]^{\mathrm{T}}$ is the vector of the received signals, $\mathbf{H}$ is the $N \times N$ circular convolution matrix constructed from the CIR coefficients given by $\mathbf{h} = [h(1), h(2), \ldots, h(N_{\mathrm{Ch}})]^{\mathrm{T}}$, and $\mathbf{n}$ is an $N \times 1$ vector of AWGN samples. The elements of $\mathbf{h}$ and $\mathbf{n}$ follow $\mathscr{CN}(0,1)$ and $\mathscr{CN}(0,\sigma_w^2)$ distributions, respectively. After substituting Eq. 3.3 in Eq. 3.6, it can be obtained as

$$\mathbf{y} = \mathbf{H}\mathbf{A}\mathbf{d} + \mathbf{n} = \widetilde{\mathbf{H}}\mathbf{d} + \mathbf{n}. \tag{3.7}$$

Eq. 3.7 enables to use JDD, which can be implemented as

$$\hat{\mathbf{d}} = \mathbf{B}\mathbf{y}. \tag{3.8}$$

Here, $\mathbf{B}$ is a $KM \times KM$ receiver matrix. There are mainly two options for $\mathbf{B}$. The ZF receiver $\mathbf{B}_{\mathrm{ZF}} = \widetilde{\mathbf{H}}^{-1}$ removes any self-interference completely but it enhances the noise. The MMSE receiver $\mathbf{B}_{\mathrm{MMSE}} = \left(\mathbf{R}_n^2 + \widetilde{\mathbf{H}}^{\mathrm{H}}\widetilde{\mathbf{H}}\right)^{-1}\widetilde{\mathbf{H}}^{\mathrm{H}}$, where $\mathbf{R}_n^2$ is a covariance matrix of the noise, makes a trade-off between self-interference and noise enhancement. Then, original information bits are retrieved after demapping and decoding stages.

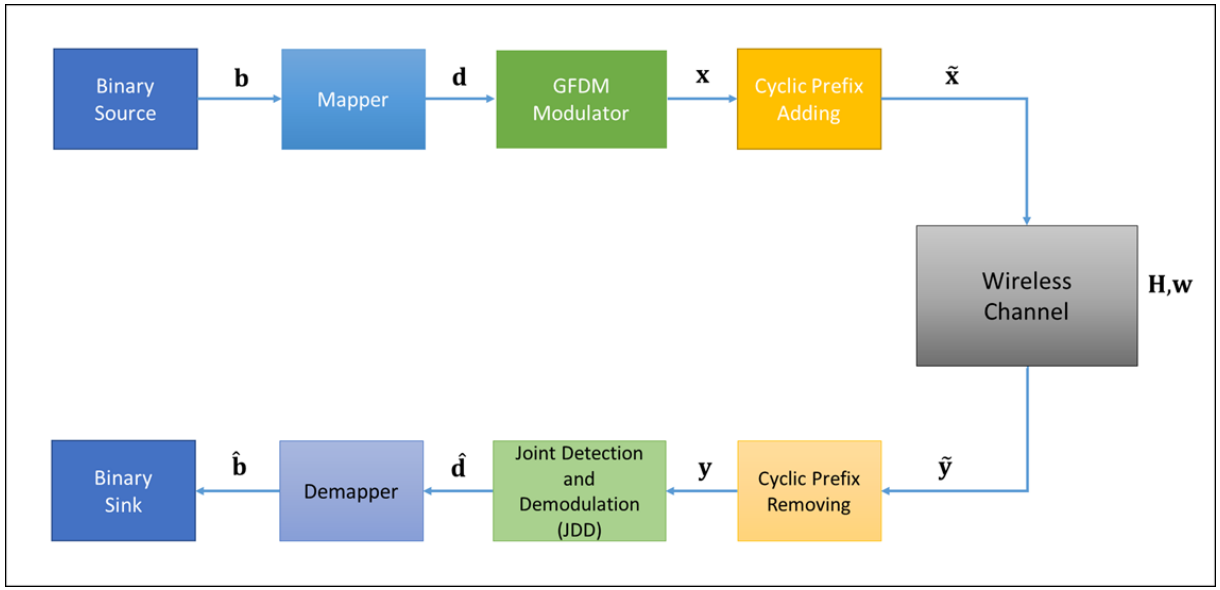

Figure 3.1 : Block Diagram of the GFDM transceiver.

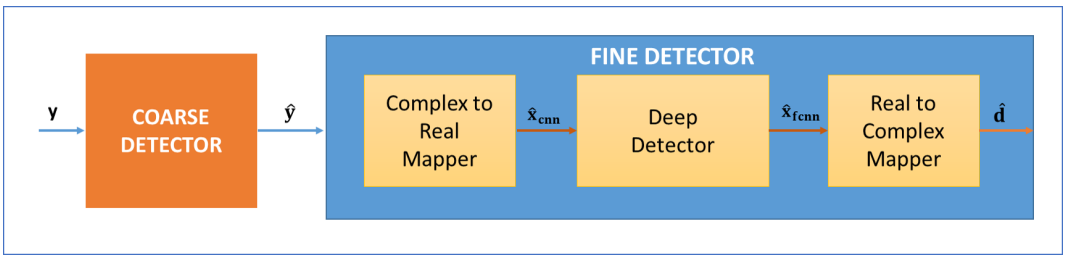

Figure 3.2 : Block Diagram of the DL-aided JDD.

3.2 Deep Detection and Demodulation for GFDM

The block diagram of the proposed DL-aided JDD scheme proposed for JDD block of the GFDM receiver is shown in Fig 3.2. In [20], it is stated that, while using neural networks for detecting communication signals, estimating the transmitted signal from very beginning may suffer from slow convergence. Therefore, in [20], a cascaded detection approach has been proposed. Inspired from [20], two-stage detection and demodulation for GFDM receiver has been proposed.

The first stage of the proposed detector is coarse detection. In this stage, thanks to system model in Eq. 3.7, modified received signal $\hat{\mathbf{y}} = \mathbf{By}$ is obtained by using well-known linear detectors such as ZF and MMSE.

The second stage of the proposed detector uses deep neural network to implement fine detection, which is expressed as

$$\hat{\mathbf{d}} = \theta(\hat{\mathbf{y}}). \tag{3.9}$$

Here, θ includes the first part of the fine detector trainable parameters, which is CNN parameters (θ_{CNN}), as well as second part of the fine detector trainable parameters, which is FCNN parameters (θ_{FCNN}). One of the challenging problems faced by deep detection is to handle complex numbers. Currently, using complex numbers in neural networks is not yet supported by any popular DL frameworks. In order to use common tools for DL, complex values have to be expressed as real values without losing relationship between real and imaginary parts of the complex numbers. The first part of the fine detector performs complex to real mapping using CNN, which can take multi-dimensional input. The complex to real mapper convolves the received signal $\mathbf{y}$

with the kernel filter $\mathbf{u}_p = \begin{bmatrix} u_{p,R} & u_{p,I} \end{bmatrix}$, adds bias $\mathbf{c}_p$, for $p = 1,...P$, with stride 1, and the modified received signal can be expressed as

$$\check{y}_p(n) = \text{Relu}(u_{p,R} * \Re(y(n)) + u_{p,I} * \Im(y(n)) + c_p), \tag{3.10}$$

where Relu is an activation function, for $n = 0,...N-1$. Here $\mathbf{u}_p$ and $\mathbf{c}_p$ are called complex to real mapper trainable parameters. The second part of the fine detector performs deep detection by using FCNN. First, FCNN based deep detector can be constructed differently with non-trainable parameters, e.g., number of layers, batch size, different optimizer, activation functions, which affect the training duration and accuracy. Second, the deep detector gets the output of the complex to real mapper and performs deep detection by using $\theta_{FCNN} = \{\mathbf{W}, \mathbf{b}\}$ trainable parameters, where $\mathbf{W} = \begin{bmatrix} \mathbf{w}_1^{\mathrm{T}}, \mathbf{w}_2^{\mathrm{T}}, ..., \mathbf{w}_L^{\mathrm{T}} \end{bmatrix}$ contains weights parameters and $\mathbf{b} = [b_1, b_2, \ldots, b_L]$ contains bias parameters, L indicates the number of layers. The number of neurons in each layer can be different, hence, weight parameters of any layer represents $\mathbf{w}_l = \begin{bmatrix} w_l(1), w_l(2), ..., w_l(T_l) \end{bmatrix}$, where T_l represents the number of neurons in the l-th layer. First layer of the FCNN gets the output of complex to real mapper $\hat{\mathbf{x}}_{cnn}$ and generates the output

$$\mathbf{e}_1 = \text{Relu}(\mathbf{w}_1 \hat{\mathbf{x}}_{cnn} + b_1). \tag{3.11}$$

Then, the second layer gets the $\mathbf{e}_1$ and generates the output

$$\mathbf{e}_2 = \text{Relu}(\mathbf{w}_2 \mathbf{e}_1 + b_2). \tag{3.12}$$

This process continues until the last layer, however tanh, which is suitable for QAM modulations, is used as the last layer activation function instead of Relu. After that, the output of the FCNN can be obtained as

$$\hat{\mathbf{x}}_{fcnn} = \begin{bmatrix} \Re(x(0)), ..., \Re(x(N-1)), \Im(x(0)), ..., \Im(x(N-1)) \end{bmatrix}. \tag{3.13}$$

Finally, the third part of the fine detector performs real to complex mapping by arranging the output of the FCNN and constructs the estimated GFDM block $\hat{\mathbf{d}}$.

3.3 Numerical Results for GFDM

In this section, the BER performance of the proposed DL aided GFDM receiver has been evaluated by computer simulations for Rayleigh fading with EPA channel model

Table 3.1 : GFDM Simulation Parameters

Description	*Parameter*	*Value*
# subcarriers	K	32
# subsymbols	M	3
Pulse shaping filter	g	RC
Roll-off factor	a	0.5
Length of cyclic prefix	N_{CP}	32
# channel taps for EPA channel	N_{Ch}	7

[38]. GFDM parameters used in the simulations are given in Table 3.1. The chosen pulse shape for the GFDM prototype filter is the RC filter with a roll-off factor (a) of 0.5. For the coarse detection stage, MMSE and ZF linear detectors are used. For the fine detection stage, model parameters are shown in Table 3.2. According to these parameters, fine detector models are constructed as shown in Table 3.3. Here, while the first two layers implement complex to real mapping, the rest of the layers implement deep detection. T_l is shown as output shape column in Table 3.3. There is no clear study of setting the training or testing SNR for DL-aided detection. The detection SNR range for simulations is 0 dB to 14 dB with 2 dB step. Accordingly, training SNR range is determined between 7 dB to 14 dB with 1 dB step. Two common optimizers, namely Adam [37] and Adadelta [39], are used. Adam optimizer is used as gradient descent algorithms. Before the start of training, θ is initialized uniformly. Training process takes from 1200 epoch. Fine detector model is constructed using Keras [40] (back-end Tensorflow-GPU [41]) and trained on Google Colab, providing GPUs in the cloud environment. For MMSE coarse detection, training data consist of 16×10^4 GFDM symbols and testing data consist of 9×10^4 symbols. For ZF-based coarse detection, training data consist of 4×10^5GFDM symbols and testing data consist of 9×10^4 symbols. The uniform distribution of the data to be trained is important for proper learning. Therefore, training data is shuffled before training.

Fig. 3.3 compares the BER performance of the MMSE-JDD and the DL-aided JDD with MMSE coarse detector for BPSK transmission. From Fig. 3.3, it is observed that the DL-aided JDD with MMSE coarse detector provides approximately 4 dB better BER performance than MMSE-JDD for Adam optimizer. Also, BER performance gains of the DL-aided JDD with MMSE coarse detector is increased to 6 dB for Adadelta optimizer.

Table 3.2 : Fine Detector Model Parameters for GFDM

Description	*Parameter*	*Value*
# Kernel Filter	P	96
# Layer	L	7
Learning Rate	lr	0.0001
Dropout Rate	r	0.1
Batch Size	B	1000

Table 3.3 : Fine Detector Model Summary for GFDM

Layer	*Output Shape*	*Activation Func.*
Input	(B,N)	None
Conv2d+Dropout(r)	(B,N,2,N)	Relu
Flatten+Dropout(r)	(B,$N^2\times$ 2)	Relu
Dense+Dropout(r)	(B,1000)	Relu
Dense+Dropout(r)	(B,1000)	Relu
Dense+Dropout(r)	(B,1000)	Relu
Dense+Dropout(r)	(B,1000)	Relu
Dense+Dropout(r)	(B,1000)	Relu
Dense+Dropout(r)	(B,1000)	Relu
Dense+Dropout(r)	(B,N$\times$2)	tanh

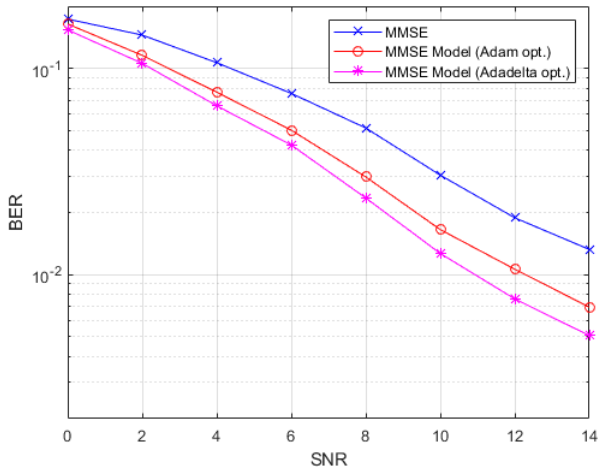

Figure 3.3 : BER Performance of MMSE-JDD and DL-aided JDD with MMSE Coarse Detector for BPSK Transmission.

Fig. 3.4 displays the BER performance of the ZF-JDD and the GFDM-ZF, the DL-aided JDD with ZF coarse detector for BPSK transmission. From Fig. 3.4, it is observed that the DL-aided JDD with ZF coarse detector provides approximately 5 dB

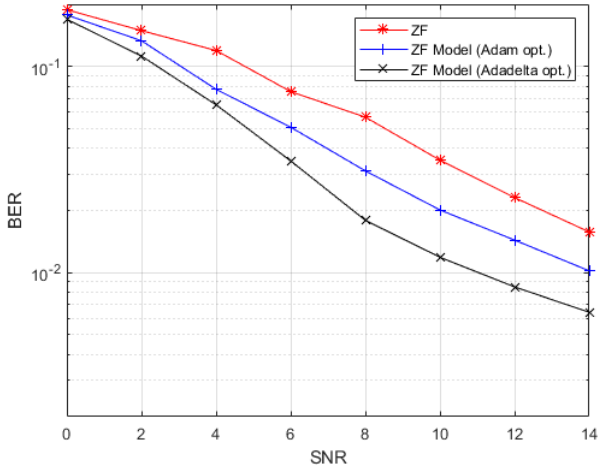

Figure 3.4 : BER Performance of ZF-JDD and DL-aided JDD with ZF Coarse Detector for BPSK Transmission.

better BER performance than ZF-JDD for Adam optimizer. For Adadelta optimizer, the DL-aided JDD with ZF coarse detector provides 3 dB additional BER gain.

4. GENERALIZED FREQUENCY DIVISION MULTIPLEXING WITH INDEX MODULATION

In this stage, GFDM-IM scheme has been examined and deep learning aided GFDM-IM detection scheme has been proposed. In Section I, the system model for GFDM-IM is presented. In Section III, Deep-SMX-IM is presented. Numerical results are given in Section III.

4.1 System Model for GFDM-IM

The block diagram of the GFDM-IM transceiver has been shown in Fig 4.1. Consider a GFDM symbol with M subsymbols each consisting of K subcarriers, the m-th subsymbol is partitioned into L IM blocks, each containing $u = K/L$ subcarrier positions. In an IM block, only v out of u subcarrier positions are selected as active and used to transmit QAM symbols from Q-ary signal constellation $\mathscr{S}$ with Q elements. Thus, an IM block can transmit a p-bit binary message $\mathbf{s}_m^l = \left[s_m^l(1), s_m^l(2), \ldots, s_m^l(p)\right]^T$. In each IM block, $p_q = v\log_2(Q)$ bits of incoming p-bits sequence are used as QAM-bits. The remaining $p_i = \lfloor \log_2(C(u,v)) \rfloor$ bits of this sequence are used to determine the active subcarrier positions. Therefore, it can be obtained $\alpha = 2^{p_i}$ possible realizations. Here, $C(\mu, \nu)$ is the binomial coefficient and $\lfloor \cdot \rfloor$ denotes the floor function. Note that active subcarrier positions can be determined using a look-up table or combinatorial methods [8]. As a result, IM blocks $\mathbf{d}_m^l = \left[d_m^l(1), d_m^l(2), \ldots, d_m^l(u)\right]^T$, where $d_m^l(\gamma) \in \{0, \mathscr{S}\}$, is constructed according to p input bits [12]. Then, IM blocks are first concatenated to obtain the GFDM-IM subsymbol $\mathbf{d}_m = [d_{0,m}, d_{1,m}, \ldots, d_{K-1,m}]$ and the resulting GFDM-IM subsymbols are combined to form the GFDM-IM symbol

$$\mathbf{d} = [d_{0,0}, \ldots, d_{K-1,0}, d_{0,1}, \ldots, d_{K-1,1}, \ldots, d_{K-1,M-1}], \tag{4.1}$$

where $d_{k,m} \in \{0, \mathscr{S}\}$, for $k = 0, \ldots, K-1, m = 0, \ldots, M-1$, is the data symbol of k-th subcarrier on m-th subsymbol. After that, the GFDM-IM symbol $\mathbf{d}$ is modulated using

a GFDM modulator and the resulting GFDM transmit signal can be expressed as

$$\mathbf{x} = \mathbf{A}\mathbf{d}, \tag{4.2}$$

where $\mathbf{A}$ is an $N \times N$ GFDM modulation matrix [4], $N = KM$. Finally, a CP with length N_{CP} is attached to $\mathbf{x}$ and the resulting vector $\tilde{\mathbf{x}} = \left[\mathbf{x}(KM - N_{\mathrm{CP}} + 1 : KM)^T, \mathbf{x}^T\right]^T$ is transmitted over a frequency-selective Rayleigh fading channel.

At the receiver side, assuming that perfect synchronization is ensured, CP is longer than the tap length of the channel (N_{Ch}) and the wireless channel stays constant through the broadcast of a GFDM symbol, after the removal of CP the received signal vector $\mathbf{y}$ can be obtained as

$$\mathbf{y} = \mathbf{H}\mathbf{x} + \mathbf{n} \tag{4.3}$$

where $\mathbf{y} = [y(0), y(1), \ldots, y(N-1)]^{\mathrm{T}}$ denotes the vector of the received signals, $\mathbf{H}$ represents the $N \times N$ circular convolution matrix constructed from the CIR coefficients given by $\mathbf{h} = [h(1), h(2), \ldots, h(N_{\mathrm{Ch}})]^{\mathrm{T}}$, and $\mathbf{n}$ is an $N \times 1$ vector of AWGN samples. The elements of $\mathbf{h}$ and $\mathbf{n}$ follow $\mathscr{CN}(0,1)$ and $\mathscr{CN}(0, \sigma_w^2)$ distributions, respectively. After substituting Eq. 4.2 in Eq. 4.3, it is obtained the equivalent channel of the GFDM-IM scheme as

$$\mathbf{y} = \mathbf{H}\mathbf{A}\mathbf{d} + \mathbf{n} = \widetilde{\mathbf{H}}\mathbf{d} + \mathbf{n}. \tag{4.4}$$

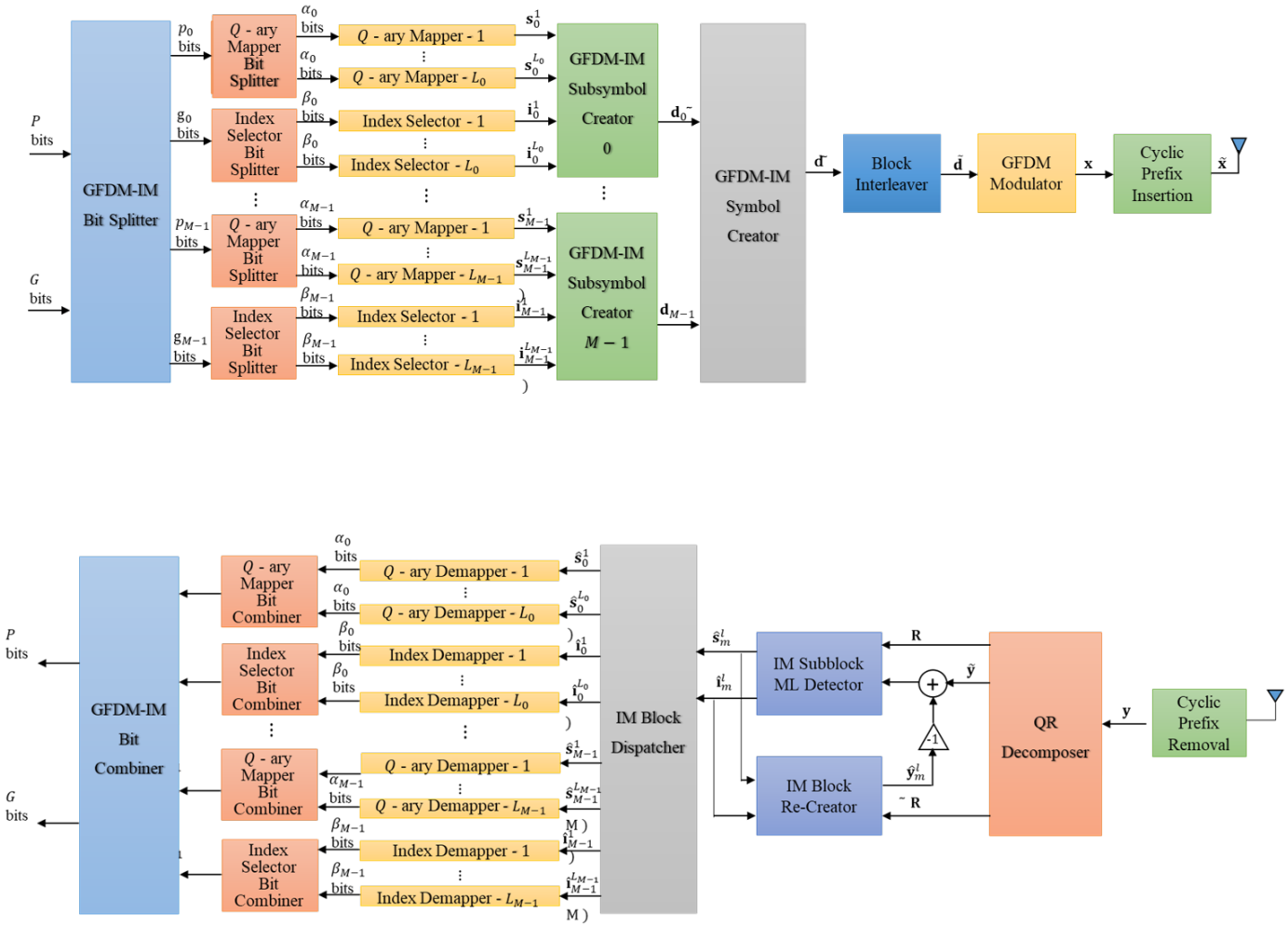

Figure 4.1 : Block Diagram of the GFDM-IM transceiver

.

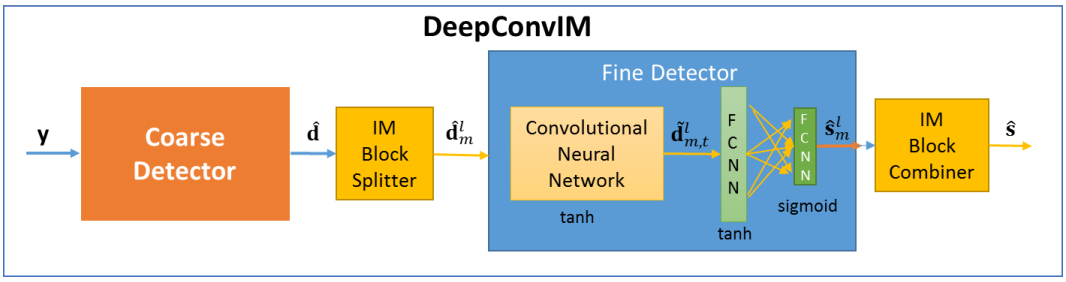

Figure 4.2 : Block Diagram of the DeepConvIM

4.2 Deep Detection and Demodulation for GFDM-IM

The block diagram of the proposed deep convolutional neural network-based joint GFDM-IM detection and demodulation scheme, termed as DeepConvIM, is shown in Fig 4.2. GFDM-IM subcarriers are non-orthogonal to each other thank to non-rectangular pulse shaping unlike OFDM-IM. Therefore, the inherent ICI prevents the frequency domain decoupling of GFDM-IM subcarriers for both SISO and MIMO transmission schemes. As a result, simultaneous detection of all subcarriers is required for optimum decision. Because this process is computationally infeasible, for the optimum detection problem of GFDM-IM, low complexity solutions are required. Inspired from [20], the proposed detector has two parts as coarse detector and fine detector. This two stage approach prevents getting stuck of neural network in a saddle point and enables the processing IM blocks independently. First, coarse detector uses ZF detector in order to process channel and GFDM modulation effects jointly. The output vector of coarse detector can be expressed as

$$\hat{\mathbf{d}} = \left(\tilde{\mathbf{H}}^H \tilde{\mathbf{H}}\right)^{-1} \tilde{\mathbf{H}}^H \mathbf{y}. \tag{4.5}$$

Since coarse detector operates on the equivalent channel of the GFDM-IM scheme, the remaining parts can handle the IM blocks individually. Therefore, fine detector processes the IM blocks independently. IM Block Splitter partitions the pre-processed received vector $\hat{\mathbf{d}}$ into IM blocks $\hat{\mathbf{d}}_m^l = \left[\hat{d}_m^l(1), \hat{d}_m^l(2), \ldots, \hat{d}_m^l(u)\right]^T$. The fine detector part of DeepConvIM uses a CNN followed by a FCNN, which is expressed as

$$\hat{\mathbf{s}}_m^l = \theta(\hat{\mathbf{d}}_\mathbf{m}^\mathbf{l}), \tag{4.6}$$

where θ represent the total of trainable parameters. The CNN part of the fine detector convolves the IM block $\hat{\mathbf{d}}_m^l$ with the kernel filter $\mathbf{a}_t = \begin{bmatrix} a_{t,R} & a_{t,I} \end{bmatrix}$, adds bias $\mathbf{c}_t$, for $t = 1,...T$, with stride 1, and the modified received IM block can be expressed as

$$\check{d}_{m,t}^l(\gamma) = \tanh(a_{t,R} * \Re(\hat{d}_m^l(\gamma)) + a_{t,I} * \Im(\hat{d}_m^l(\gamma)) + c_t), \tag{4.7}$$

where tanh is an activation function, for $\gamma = 1,...,u$. Here $\mathbf{a}_t$ and $\mathbf{c}_t$ are called convolution trainable parameters. Notice that unlike [29], DeepConvIM does not need the energy of the received signal. The FCNN part of the fine detector gets the output of the CNN and performs deep detection by using $\{\mathbf{W}, \mathbf{b}\}$ trainable parameters, where $\mathbf{W} = \begin{bmatrix} \mathbf{w}_1, \mathbf{w}_2 \end{bmatrix}$ contains weights parameters and $\mathbf{b} = [b_1, b_2]$ contains bias parameters. That is, The FCNN part uses only two fully-connected layers, hidden layer has τ nodes the output layer has p nodes as expected. The output of fine detector can be expressed as

$$\hat{\mathbf{s}}_m^l = \text{sigmoid}(\mathbf{w}_2(\tanh(\mathbf{w}_1 \check{\mathbf{d}}_{m,t}^l + b_1)) + b_2, \tag{4.8}$$

where sigmoid is an activation function. Finally, IM Block Combiner merges the output of the fine detector and forms the transmitted information bits.

The aim of the training stage of DeepConvIM is to find θ parameters in order to minimize the cost function, which calculates averages of loss function for total training datasets. Loss functions can be expressed as $(\mathbf{s}_m^l, \hat{\mathbf{s}}_m^l) = \|\mathbf{s}_m^l - \hat{\mathbf{s}}_m^l\|$. Before training, GFDM-IM simulation training data is generated and divided into batch (B). At first, the θ is randomly initialized. Throughout the training, θ is updated according to stochastic gradient descent (SGD) algorithm for every batch, which is expressed as

$$\theta_+ = \theta - \eta \bigtriangledown cost(\mathbf{s}_m, \hat{\mathbf{s}}_m), \tag{4.9}$$

where η is learning rate.

Table 4.1 : Computational Complexity of ZF, ML and DeepConvIM Detectors

Detector	*Process*	*Operation*	*Execution Count*	*Complexity (CMs)*
ZF	Forming $\widetilde{\mathbf{H}}$	$\Phi_{N\times N}{\Psi_{N\times N}}^{\dagger}$	1	$N_{\mathrm{Ch}}N^2RT$
	JDD	$\left({\Phi_{NR\times NT}}^{\mathrm{H}}\Phi_{NR\times NT}\right)^{-1}{\Phi_{N\times N}}^{\mathrm{H}}\phi_{NR\times 1}$	1	$3N^3+N^2$
	Decision	$\min\left(\left\|\phi_{u\times 1}-\psi_{u\times 1})\right\|^2\right)$	ML	$u\alpha Q^v ML$
ML	Forming $\widetilde{\mathbf{H}}$	$\Phi_{N\times N}{\Psi_{N\times N}}^{\dagger}$	1	$N_{\mathrm{Ch}}N^2$
	Decision	$\min\left(\left\|\phi_{N\times 1}-(\Phi_{N\times N}\psi_{N\times 1})\right\|^2\right)^{\dagger\dagger}$	$(\alpha Q^v)^{ML}$	$(\alpha Q^v)^{ML}(NvML+N)$
DeepConvIM	Forming $\widetilde{\mathbf{H}}$	$\Phi_{N\times N}{\Psi_{N\times N}}^{\dagger}$	1	$N_{\mathrm{Ch}}N^2$
	JDD	$\left({\Phi_{N\times N}}^{\mathrm{H}}\Phi_{N\times N}\right)^{-1}{\Phi_{N\times N}}^{\mathrm{H}}\phi_{N\times 1}$	1	$3N^3+N^2$
	CNN	$(2uFT+uT\lambda)/3^{\dagger\dagger\dagger}$	ML	$(uT(2+\lambda))ML/3$
	FCNN	$(uT\tau+\tau\lambda+\tau p+p\delta)/3^{\dagger\dagger\dagger\dagger}$	ML	$(uT\tau+\tau\lambda+\tau p+p\delta)ML/3$

† In every row of $\mathbf{H}$, which is Φ in this case, only N_{Ch} out of N elements are non-zero.
†† In ψ, only vML complex elements are nonzero.
††† λ refers to number of real multiplications required for *tanh* function.
†††† δ and τ refers to number of real multiplications required for *sigmoid* function and the number of nodes of the hidden layer of FCNN, respectively.

Table 4.2 : Summary of the Computational Complexity of ZF, ML and DeepConvIM Detectors for GFDM-IM

Detector	*Total Complexity (CMs)*
ZF	$3N^3 + N^2(1+N_{\text{Ch}}) + \alpha Q^v ML$
ML	$(\alpha Q^v)^{ML}(NvML+N) + N_{\text{Ch}}N^2$
DeepConvIM	$3N^3 + N^2(1+N_{\text{Ch}}) + (uT(2+\lambda))ML/3 + (uT\tau + \tau\lambda + \tau p + p\delta)ML/3$

Table 4.3 : A Look-up Table Example for $u = 4, v = 2$.

Bits	*Indices*	*IM block*
[0 0]	$\{1,2\}$	$\begin{bmatrix} s_\chi & s_\zeta & 0 & 0 \end{bmatrix}^T$
[0 1]	$\{2,3\}$	$\begin{bmatrix} 0 & s_\chi & s_\zeta & 0 \end{bmatrix}^T$
[1 0]	$\{3,4\}$	$\begin{bmatrix} 0 & 0 & s_\chi & s_\zeta \end{bmatrix}^T$
[1 1]	$\{1,4\}$	$\begin{bmatrix} s_\chi & 0 & 0 & s_\zeta \end{bmatrix}^T$

4.3 Complexity Analysis for GFDM-IM

Computational complexity of ZF, ML and DeepConvIM detectors has been investigated from the standpoint of number of CMs and given in Table 4.1. Here, $\Psi_{J\times I}$ and $\Phi_{J\times I}$ are used for $J \times I$ matrices, $\psi_{J\times 1}$ and $\phi_{J\times 1}$ stand for $J \times 1$ vectors. Notice that using complex numbers is not yet supported by any popular deep learning frameworks and FCNN part of DeepConvIM operates on real numbers thanks to CNN part. Since one complex multiplication can be carried out with at least three real multiplications, the number of multiplications belonging to neural networks parts of DeepConvIM are divided to three in order to refer them as complex multiplications. The summary of the results is given in Table 4.2. From Table 4.2, it is observed that while ZF and ML detectors have the lowest and the highest complexity, respectively, DeepConvIM provides an intermediate solution with regard to computational complexity.

4.4 Numerical Results for GFDM-IM

In this section, the BER performance of DeepConvIM has been compared to ZF and ML detection methods. The chosen pulse shape for the GFDM prototype filter is the RC filter with a roll-off factor (a) of 0.5. The active subcarrier indices are selected

Table 4.4 : The Total Number of CMs for ZF, ML and DeepConvIM Detectors for GFDM-IM

Configuration	*ZF*	*DeepConvIM*	*ML*
BPSK, $K = 32, M = 1$	1.07×10^5	1.18×10^5	2.33×10^{12}
4-QAM, $K = 32, M = 1$	1.09×10^5	1.56×10^5	1.48×10^{22}
16-QAM, $K = 32, M = 1$	2.37×10^5	4.20×10^5	4.15×10^{36}
BPSK, $K = 8, M = 1$	2.08×10^3	5.15×10^3	1.07×10^4
BPSK, $K = 8, M = 3$	4.61×10^4	5.54×10^4	5.23×10^9

Table 4.5 : Fine Detector Model Parameters for GFDM-IM

Description	*Parameter*	*Value*
# Kernel Filter (for BPSK transmission)	T	16
# Kernel Filter (for 4-QAM transmission)	T	32
# Kernel Filter (for 16-QAM transmission)	T	64
# Nodes of Hidden Layer (for BPSK transmission)	τ	64
# Nodes of Hidden Layer (for 4-QAM transmission)	τ	128
# Nodes of Hidden Layer (for 16-QAM transmission)	τ	256
Learning Rate	lr	0.0008
Batch Size	B	1000

Table 4.6 : Fine Detector Model Summary for GFDM-IM

Layer	*Output Shape*	*Activation Func.*
Input	(B,2,u,1)	None
Conv2d	(B,1,u,T)	tanh
Flatten	(B,uT)	None
Dense	(B,τ)	tanh
Dense	(B,p)	sigmoid

using the lookup table in Table 4.3. Fine detector model parameters and summary are given in Table 4.5 and 4.6, respectively. During training stage, SNR is set to 15dB, Adam optimizer [37], which is SGD-based, is used, and the learning rate is set to 8×10^{-4}. The DeepConvIM model is trained in a short time, 60 epochs is enough to get significant results. A GFDM-IM training data set, including 16×10^4 symbols, and a GFDM-IM testing data set, including 3×10^4 symbols are generated for each SNR value regarding $K = 32$. For $K = 8$, training data and testing data include 32×10^4 and 6×10^4 GFDM-IM symbols, respectively.

DeepConvIM model is constructed using Keras [40] (back-end Tensorflow [41]) and trained on Google Colab, providing tensor processing units (TPUs) in the cloud environment.

Fig. 4.3 compares the BER performance of the ZF and the DeepConvIM with ZF coarse detector for BPSK transmission when $K = 32$ and $M = 1$. From Fig. 4.3, it is observed that the DeepConvIM provides approximately 6 dB better BER performance than ZF at a BER value of 10^{-4} .

Fig. 4.4 compares the BER performance of the ZF and the DeepConvIM with ZF coarse detector for 4-QAM and 16-QAM transmissions when $K = 32$ and $M = 1$. From Fig. 4.4, it is observed that the DeepConvIM provides approximately 4.5 and 1 dB better BER performance than ZF for 4-QAM and 16-QAM transmissions, respectively, at a BER value of 10^{-4}.

Fig. 4.5 compares the BER performance of the ZF, ML and the DeepConvIM with ZF coarse detector for BPSK transmission, when $K = 8$, $M = (1,3)$. From Fig. 4.5, at a BER value of 10^{-4}, while DeepConvIM provides 6 dB BER improvement with respect to ZF detector for $M = 3$, the BER improvement of DeepConvIM with ZF coarse detector with respect to ZF detector is increased to 8 dB when $M = 1$. Also, ML detector has 8 dB BER improvement with respect to DeepConvIM when $M = 1$.

From Fig. 4.3 and 4.4, it is observed that as the modulation order increases, the learning capacity of the model decreases. From Fig. 4.4, it is observed that when the number of subsymbols increases, performance of the model decreases. On the other hand, from Fig. 4.3 and 4.5, it is observed that when the number of subcarriers decreases, performance of the model increases. The number of CMs needed by the detectors in Fig. 4.3, 4.4 and 4.5 are given in Table 4.4. As mentioned earlier, DeepConvIM can be evaluated as a intermediate solution regarding computational complexity.

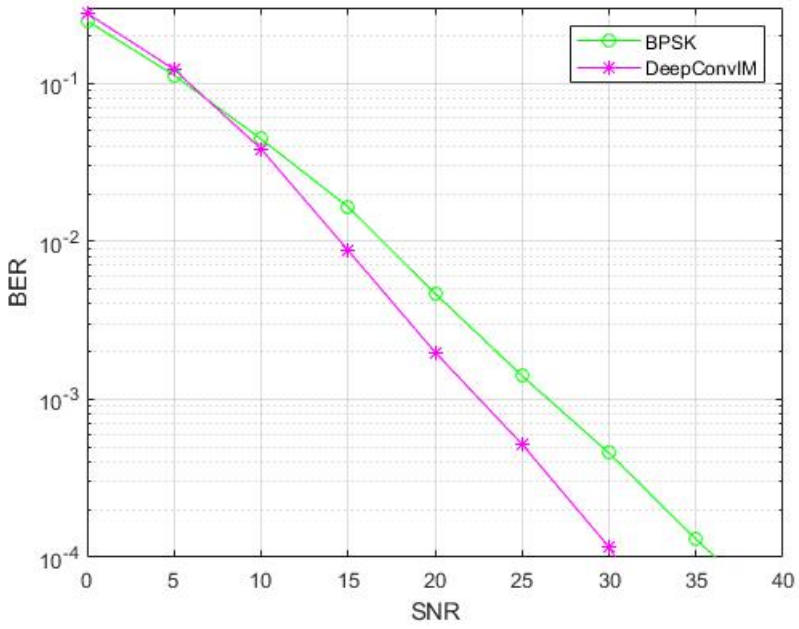

Figure 4.3 : BER Performance of ZF and DeepConvIM with ZF Coarse Detector for BPSK transmission, ($K = 32$, $M = 1$)

.

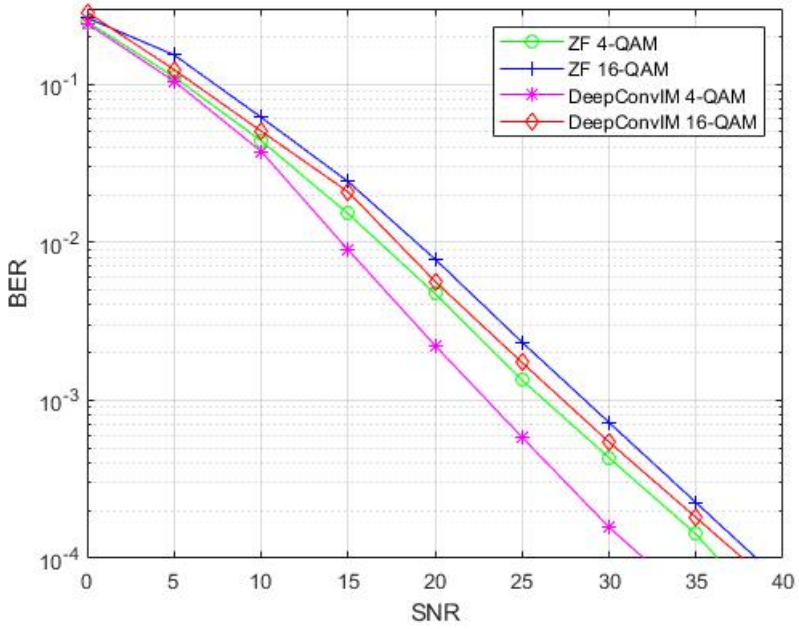

Figure 4.4 : BER Performance of ZF and DeepConvIM with ZF Coarse Detector for 4-QAM and 16-QAM transmissions ($K = 32$, $M = 1$).

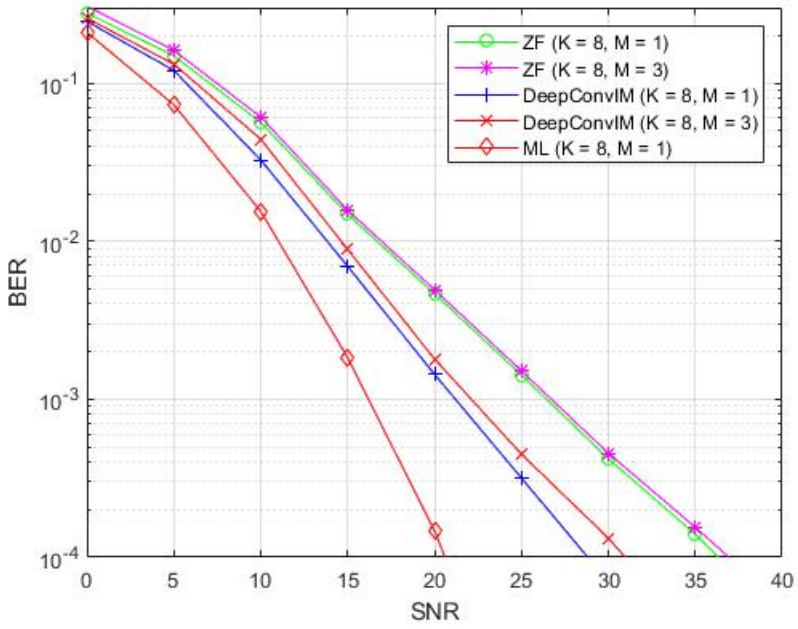

Figure 4.5 : BER Performance of ZF and DeepConvIM with ZF Coarse Detector for BPSK Transmission ($K = 8$, $M = (1\ ,\ 3)$).

5. SPATIAL MULTIPLEXING WITH INDEX MODULATION

In this stage, SMX-IM for GFDM and OFDM scheme has been examined and deep learning aided SMX-IM detection scheme has been proposed. In Section I, the system model for SMX-GFDM-IM and SMX-OFDM-IM is presented. In Section II, Deep-SMX-IM is presented. Numerical results are given in Section III.

5.1 System Model for SMX-IM

Consider a MIMO system employing T transmit and R receive antennas. The block diagram of the SMX-GFDM-IM transmitter is given in Fig. 5.1. The MIMO-GFDM-IM transmitter gets a total of PT information bits enter for the transmission of each frame. A GFDM symbol, each consisting of M subsymbols with K subcarriers, is partitioned into L IM blocks, each containing $u = MK/L$ subcarrier positions. In an IM block, only v out of u subcarrier positions are selected as active and used to transmit QAM symbols from Q-ary signal constellation $\mathscr{S}$ with Q elements. Thus, an IM block can transmit a p-bit binary message $\mathbf{s}_t^l = \left[s_t^l(1), s_t^l(2), \ldots, s_t^l(p)\right]$, for $l = 1, \ldots, L$ and $P = pL$. In each IM block, $p_q = v\log_2(Q)$ bits of incoming p-bits sequence are used as QAM-bits. The remaining $p_i = \lfloor \log_2(C(u,v)) \rfloor$ bits of this sequence are used to determine the active subcarrier positions with using a look-up table or combination methods [8]. Therefore, $\lambda = 2^{p_i}$ possible realizations is obtained as seen from 5.2. Here, $C(\mu, \nu)$ is the binomial coefficient. As a result, IM blocks $\mathbf{d}_t^l = \left[d_t^l(1), d_t^l(2), \ldots, d_t^l(u)\right]^T$, where $d_t^l(\gamma) \in \{0, \mathscr{S}\}$, is constructed according to p input bits [12]. Then, the resulting IM blocks are merged to form the GFDM-IM symbol

$$\mathbf{d_t} = \left[d_{t,0,0}, \ldots, d_{t,K-1,0}, d_{t,0,1}, \ldots, d_{t,K-1,1}, \ldots, d_{t,K-1,M-1}\right] \tag{5.1}$$

where $d_{t,k,m} \in \{0, \mathscr{S}\}$, for $k = 0, \ldots, K-1, m = 0, \ldots, M-1, t = 1, \ldots, T$ is the data symbol of k-th subcarrier on m-th subsymbol of a GFDM symbol belonging to t-th transmit antenna. After that, the GFDM-IM symbol $\mathbf{d}_t$ is modulated using a GFDM

modulator and the resulting GFDM transmit signal can be obtained as

$$\mathbf{x_t} = \mathbf{A}\mathbf{d_t}, \tag{5.2}$$

where $\mathbf{A}$ denotes an $N \times N$ GFDM modulation matrix [4], $N = MK$. Finally, CP with length N_{CP} is attached to $\mathbf{x_t}$ and the resulting vector $\tilde{\mathbf{x}}_\mathbf{t} = \left[\mathbf{x_t}\left(MK - N_{\mathrm{CP}} + 1 : MK\right)^T, {\mathbf{x_t}}^T\right]^T$ is transmitted over a frequency-selective Rayleigh fading channel. At the receiver side, assuming that perfect synchronization is ensured, CP is longer than the tap length of the channel (N_{Ch}) and the wireless channel remains constant through the broadcast of a GFDM symbol, the received signal can be obtained as

$$\begin{bmatrix} \mathbf{y}_1 \\ \vdots \\ \mathbf{y}_R \end{bmatrix} = \begin{bmatrix} \mathbf{H}_{1,1}\mathbf{A} & \dots & \mathbf{H}_{T,1}\mathbf{A} \\ \vdots & \ddots & \vdots \\ \mathbf{H}_{R,1}\mathbf{A} & \dots & \mathbf{H}_{R,T}\mathbf{A} \end{bmatrix} \qquad \begin{bmatrix} \mathbf{d}_1 \\ \vdots \\ \mathbf{d}_T \end{bmatrix} + \begin{bmatrix} \mathbf{n}_1 \\ \vdots \\ \mathbf{n}_R \end{bmatrix} \tag{5.3}$$

after the removal of CP. Here, $\mathbf{y}_R = [y_r(0), y_r(1), \dots, y_r(N-1)]^{\mathrm{T}}$ represents the vector of the received signals, $\mathbf{H}_{r,t}$, for $t = 1, \dots, Tr = 1, \dots, R,$, denotes the $N \times N$ circular convolution matrix constructed from the CIR coefficients given by $\mathbf{h}_{r,t} = [h_{r,t}(1), h_{r,t}(2), \dots, h_{r,t}(N_{\mathrm{Ch}})]^{\mathrm{T}}$, and $\mathbf{n}_r$ is an $N \times 1$ vector of AWGN samples. The elements of $\mathbf{h}_{r,t}$ and $\mathbf{n}_r$ follow $\mathscr{CN}(0,1)$ and $\mathscr{CN}(0,\sigma_w^2)$ distributions, respectively. After substituting Eq. 5.2 in Eq. 5.3, the equivalent channel of the GFDM-IM scheme is obtained as

$$\mathbf{y} = \widetilde{\mathbf{H}}\mathbf{d} + \mathbf{n}. \tag{5.4}$$

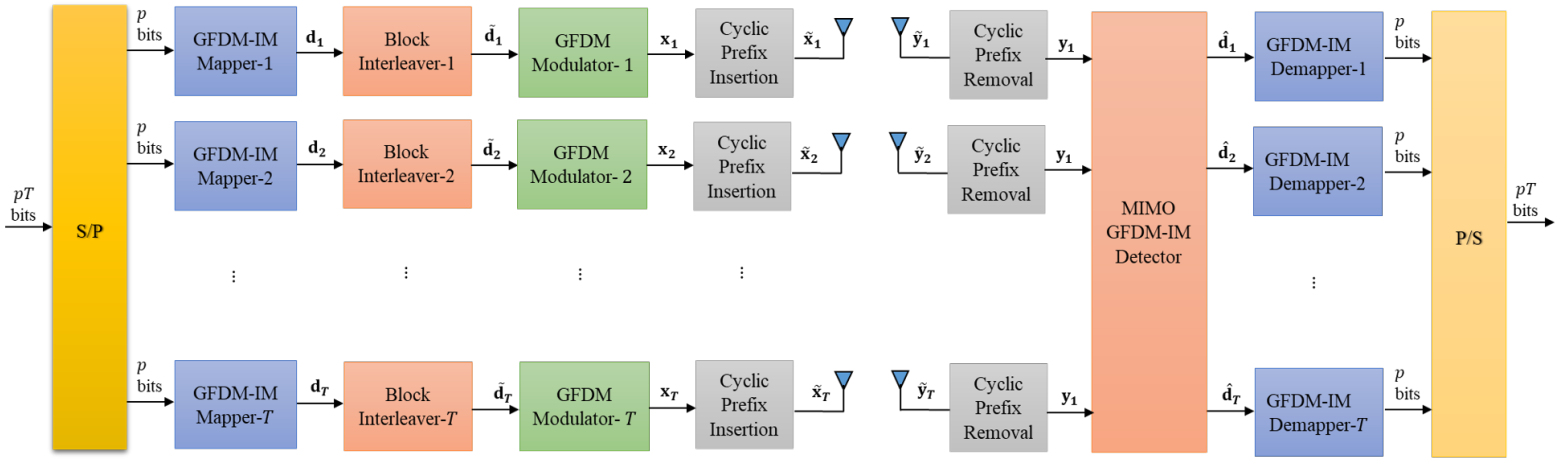

Figure 5.1 : Block Diagram of the SMX-GFDM-IM Transceiver.

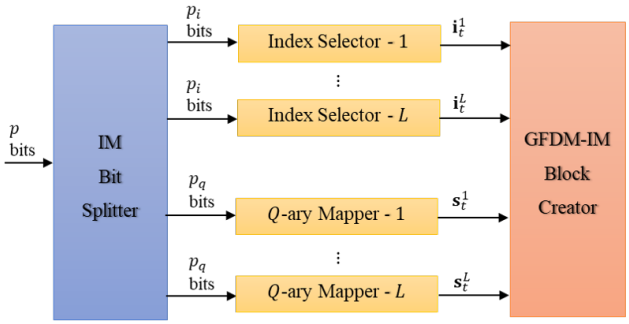

Figure 5.2 : GFDM-IM Mappers at Each Branch of the Transmitter.

5.2 Deep Detection and Demodulation for SMX-IM

The block diagram of the proposed deep learning-aided data detection of spatial multiplexing scheme, termed as Deep-SMX-IM, is given in Fig 5.3. The channel information is assumed to be perfectly known at the receiver. The proposed detector is built as two stages as coarse detector and fine detector. It also has two intermediate steps for regularizing coarse detector output and fine detector outputs, which are SMX-IM Block Splitter and Combiner, respectively. As a first stage, coarse detector applies ZF detector to handle channel and GFDM modulation effects together and the coarse detector's output can be given by

$$\begin{bmatrix} \psi_1 \\ \psi_2 \\ \vdots \\ \psi_T \end{bmatrix} = \left(\widetilde{\mathbf{H}}^H \widetilde{\mathbf{H}}\right)^{-1} \widetilde{\mathbf{H}}^H \mathbf{y}, \tag{5.5}$$

where $\psi_t = [\psi_t^{1^T}, \psi_t^{2^T}, ..., \psi_t^{L^T}]^T$, for $t = 1, ...T$ and for $l = 1, ...L$, ψ_t^l denotes a $u \times 1$ vector. After coarse detector, ψ_t^l are subdivided into sub-block IM form by SMX-IM Block Splitter and the resulting matrix can be expressed as

$$\mathbf{\Psi}^l = \begin{bmatrix} \psi_1^l(1) & \dots & \psi_1^l(u) \\ \vdots & \ddots & \vdots \\ \psi_T^l(1) & \dots & \psi_T^l(u) \end{bmatrix}. \tag{5.6}$$

The fine detector stage of Deep-SMX-IM is built by using CNN and FCNN, respectively. The fine detector's CNN part convolves the subblock IM block $\mathbf{\Psi}^l$ with the kernels $\mathbf{w}^f = \left[w_1^f, \dots, w_{2T}^f\right]$ adds bias $\mathbf{c}_f$ for $f = 1, ...F$ and stride 1, and the

modified received sub-block IM form is obtained as

$$\theta_f^l(\gamma) = \mathbf{f_{tanh}}(\Re(\psi_1^l(\gamma) * w_1^f) + \Im(\psi_1^l(\gamma)) * w_2^f + \ldots + \Re(\psi_T^l(\gamma) * w_{2T-1}^f) + \Im(\psi_T^l(\gamma)) * w_{2T}^f + c_f)$$

for $f = 1, ..., F$ and $\gamma = 1, ..., u$. Note that since complex numbers are not supported by any DL framework yet, real and imaginer parts of the received signals are processed separately. The CNN part repeats the convolution operation for F different kernel filters. The output from CNN can be obtained as

$$\mathbf{\Theta}^l = \begin{bmatrix} \theta_1^l(1) & \theta_1^l(2)\ldots & \theta_1^l(u) \\ \vdots & \ddots & \vdots \\ \theta_F^l(1) & \ldots & \theta_F^l(u) \end{bmatrix}. \tag{5.7}$$

After that, $\mathbf{\Theta}^l$ is converted into a vector by flattening process and the resulting vector can be expressed as $\theta^l = [\theta_1^l(1), \ldots, \theta_1^l(u), \ldots, \theta_F^l(1), \ldots, \theta_F^l(u)]^T$. The fine detector's FCNN part executes θ^l with using $\{\mathbf{a}, \mathbf{b}\}$ parameters, where $\mathbf{a} = \left[\mathbf{a}_1, \mathbf{a}_2\right]$ includes weight parameters and $\mathbf{b} = [b_1, b_2]$ contains bias parameters. This part consists of only two layers, first layer and output layer have τ and PT neurons, respectively. Fine detector's output is obtained as

$$\hat{\mathbf{s}}^l = \mathbf{f_{sigmoid}}(\mathbf{a}_2(\mathbf{f_{tanh}}(\mathbf{a}_1\theta^l + b_1)) + b_2, \tag{5.8}$$

where $\mathbf{f_{sigmoid}}, \mathbf{f_{tanh}}$ are activation functions. Finally, SMX-IM Block Combiner compose the fine detector's output into transmitted information bits. Before using the proposed Deep-SMX-IM detector, it has to be trained offline with the data which is generated at training signal-to-noise ratio (SNR) value by simulations. While training step uses fixed SNR value, testing step uses a range of SNR values. Deciding training SNR value has a key role against overfit. The training offline executes on total trainable parameters, which consists of $\mathbf{w}_f, \mathbf{c}_f, \alpha, \beta$, for the purpose of minimizing the loss function. It can be expressed as $loss(\mathbf{s}^l, \hat{\mathbf{s}}^l) = \|\mathbf{s}^l - \hat{\mathbf{s}}^l\|$. In the training stage, total trainable parameters are randomly initialized at first. Throughout the training, stochastic gradient descent algorithm executes on these parameters, it can be obtained as

$$\varepsilon_+ = \varepsilon - \eta \bigtriangledown loss(\mathbf{s^l}_B, \hat{\mathbf{s}^l}_B), \tag{5.9}$$

where ε, B, η represent total trainable parameters, learning rate and batch size respectively.

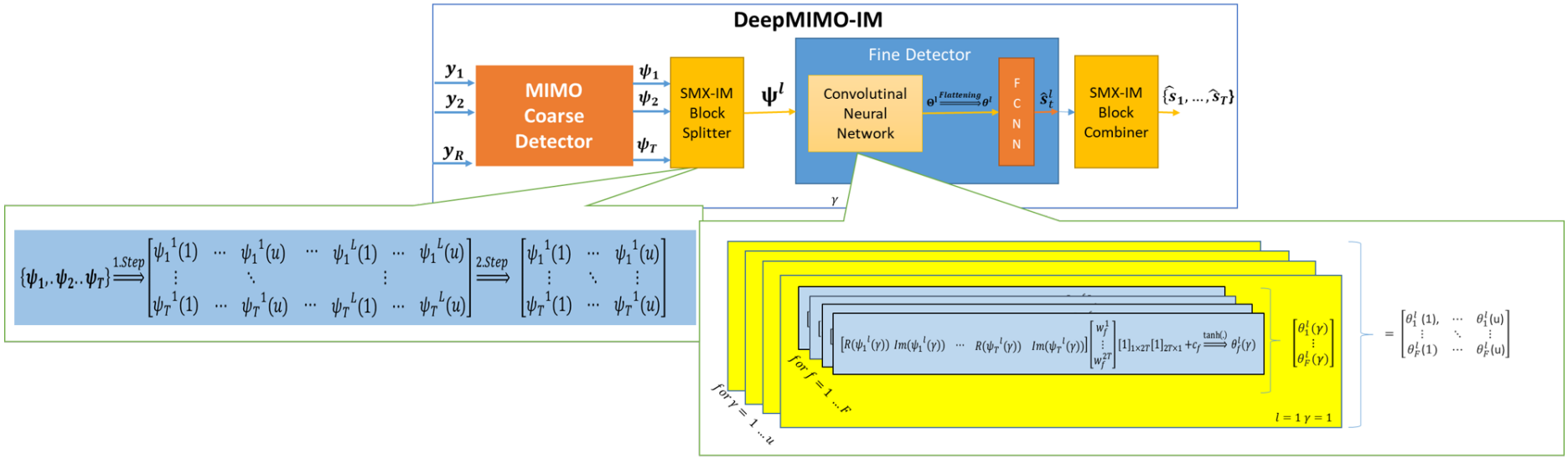

Figure 5.3 : Block Diagram of the Deep-SMX-IM Receivers.

5.3 Complexity Analysis for SMX-IM

Computational complexity of ZF, ML and DeepSMX-IM detectors is investigated from the standpoint of number of CMs and given in Table 5.1. Here, $\Psi_{J\times I}$ and $\Phi_{J\times I}$ are used for $J \times I$ matrices, $\psi_{J\times 1}$ and $\phi_{J\times 1}$ stand for $J \times 1$ vectors. Notice that using complex numbers is not yet supported by any deep learning frameworks and FCNN part of DeepSMX-IM operates on real numbers thanks to CNN part. Since one complex multiplication can be carried out with at least three real multiplications, the number of multiplications belonging to neural networks parts of Deep-SMX-IM are divided to three in order to refer them as complex multiplications. The summary of the results is given in Table 5.2. From Table 5.2, it is observed that while ZF and ML detectors have the lowest and the highest complexity, respectively, Deep-SMX-IM provides an intermediate solution with regard to computational complexity.

5.4 Numerical Results for SMX-IM

In this section, the performance of Deep-SMX-IM detector has been evaluated for Rayleigh fading with Extended Pedestrian A (EPA) channel model [38] employing BPSK and 4-QAM modulation. The raised cosine filter is used as a GFDM prototype filter with a roll-off factor of 0.5. The following GFDM parameters are assumed $(K = 32, M = 3, N_{Ch} = 8)$. Note that, it is assumed $(K = 32, M = 1)$ for OFDM parameters. Training data including 12×10^5 IM groups, is generated at SNR 15dB according to GFDM and OFDM parameters. In Table 5.5 and 5.4 Deep-SMX-IM fine detector model parameters and summary can be seen respectively. In order to find a global minimum, stochastic gradient based Adam optimizer [37], is used with 8×10^{-4} learning rate.

Fig. 5.4 and Fig. 5.5 give comparison result between the Deep-SMX-IM for GFDM and OFDM with ZF coarse detector for 2×2 and 4×4, respectively, using BPSK transmission. As seen from Fig. 5.4, for a 2×2 MIMO configuration, it is observed that the Deep-SMX-IM for GFDM and OFDM achieves 5.5 dB better BER performance than ZF coarse detector at a BER value of 10^{-4} . In Fig. 5.5, for a 4×4 MIMO configuration, it is observed that Deep-SMX-IM for GFDM and OFDM achieves

5.5 and 6 dB better BER performance than ZF coarse detector at BER value 10^{-4}, respectively.

Fig. 5.6 and Fig. 5.7 display the BER performance of the Deep-SMX-IM for GFDM and OFDM with ZF coarse detector for 2×2 and 4×4, respectively, using 4-QAM transmissions. From Fig. 5.6, for a 2×2 MIMO configuration, it is observed that the Deep-SMX-IM for GFDM and OFDM achieves 5.5 dB better BER performance than ZF coarse detector at a BER value of 10^{-4}. In Fig. 5.7, for a 4×4 MIMO configuration, it is observed that Deep-SMX-IM for GFDM and OFDM achieves 3 dB better BER performance than ZF coarse detector at BER value 10^{-4}.

As seen from Fig. 5.4 and 5.5, as spectral efficiency and the modulation order increases, model's learning capacity decreases. However, Deep-SMX-IM continues to retain its advantage over the classical linear detector in all conceivable system parameters. In Table 5.3, the number of CMs required for Fig. 5.4 and 5.5 are provided. Notice that, while DeepConvIM in [31] has an intermediate solution for GFDM-IM, Deep-SMX-IM can be assessed as an efficient solution in terms of computational complexity.

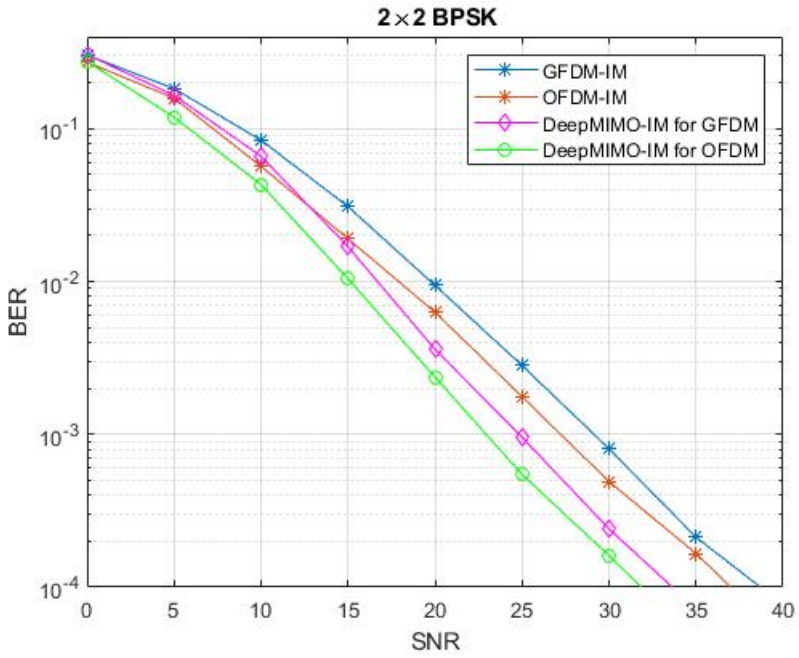

Figure 5.4 : BER Performance of ZF and Deep-SMX-IM with ZF Coarse Detector for 2×2 (BPSK)

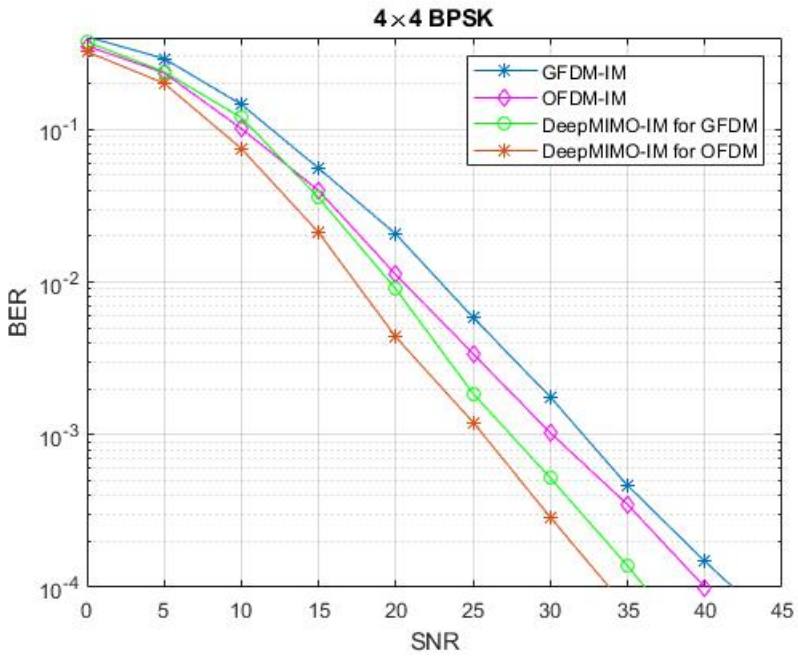

Figure 5.5 : BER Performance of ZF and Deep-SMX-IM with ZF coarse detector for 4×4 (BPSK)

.

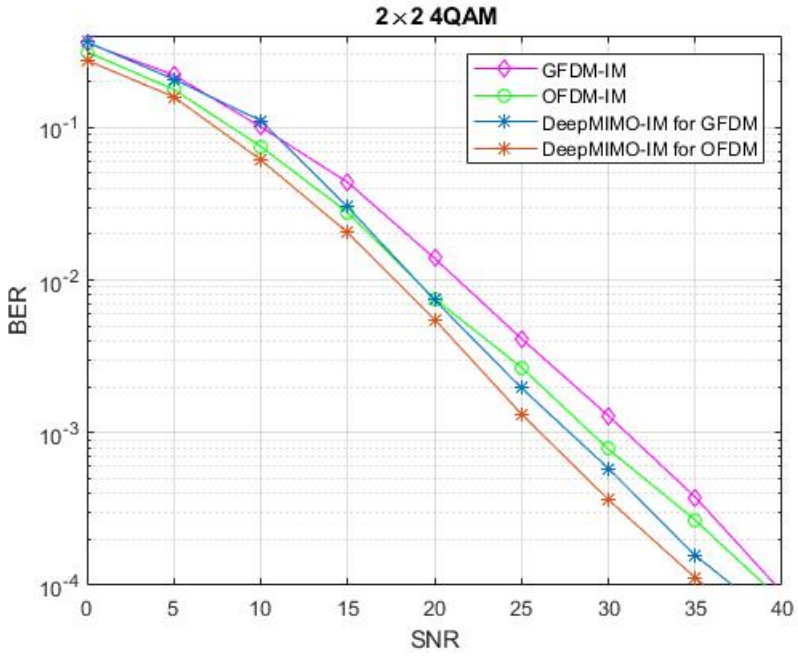

Figure 5.6 : BER Performance ZF and Deep-SMX-IM with ZF Coarse Detector for 2×2 Schemes (4-QAM)

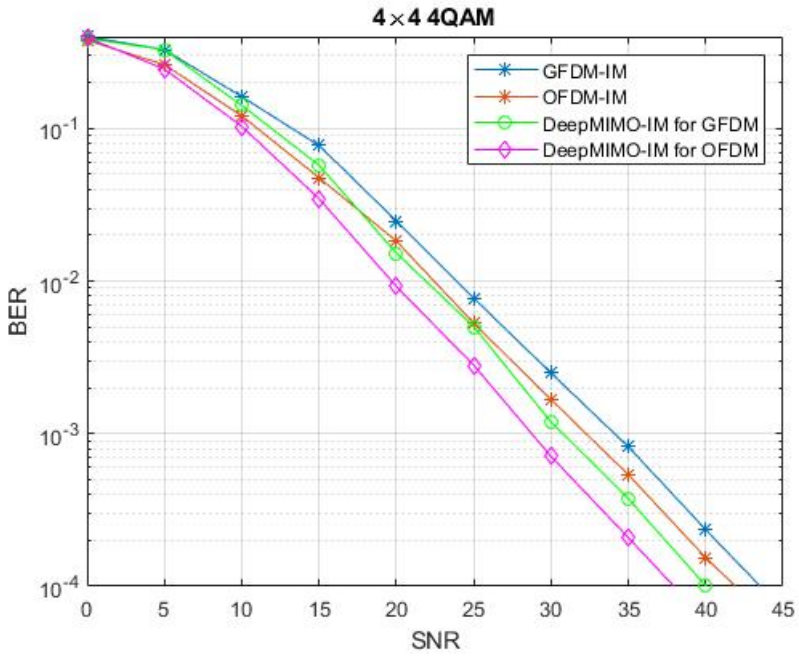

Figure 5.7 : BER Performance of ZF and Deep-SMX-IM with ZF Coarse Detector for 4×4 Schemes (4-QAM)

Table 5.1 : Computational Complexity of ZF, ML and Deep-SMX-IM Detectors

Detector	*Process*	*Operation*	*Execution Count*	*Complexity (CMs)*
ZF	Forming $\widetilde{\mathbf{H}}$	$\Phi_{N\times N}{\Psi_{N\times N}}^{\dagger}$	RT	$N_{\mathrm{Ch}}N^2RT$
	JDD	$\left({\Phi_{NR\times NT}}^{\mathrm{H}}\Phi_{NR\times NT}\right)^{-1}{\Phi_{NR\times NT}}^{\mathrm{H}}\phi_{NR\times 1}$	1	$2N^3T^2R+N^3T^3+N^2RT$
	Decision	$\min\left(\left\|\phi_{u\times 1}-\psi_{u\times 1})\right\|^2\right)$	$(N/u)cQ^vT$	NcQ^vT
RT	Forming $\widetilde{\mathbf{H}}$	$\Phi_{N\times N}{\Psi_{N\times N}}^{\dagger}$	1	$N_{\mathrm{Ch}}N^2RT$
	Decision	$\min\left(\left\|\phi_{N\times 1}-(\Phi_{N\times N}\psi_{N\times 1})\right\|^2\right)^{\dagger\dagger}$	$(cQ^v)^{TN/u}$	$(cQ^v)^{TN/u}\left((N^2TRv)/u+NT\right)$
Deep-SMX-IM	Forming $\widetilde{\mathbf{H}}$	$\Phi_{N\times N}{\Psi_{N\times N}}^{\dagger}$	RT	$N_{\mathrm{Ch}}N^2RT$
	JDD	$\left({\Phi_{NR\times NT}}^{\mathrm{H}}\Phi_{NR\times NT}\right)^{-1}{\Phi_{NR\times NT}}^{\mathrm{H}}\phi_{NR\times 1}$	1	$2N^3T^2R+N^3T^3+N^2RT$
	CNN	$(2FT+T\lambda)/3^{\dagger\dagger\dagger}$	N	$(2FT+F\lambda))N/3$
	FCNN	$(uF\tau+\tau\lambda+\tau pT+pT\delta)/3^{\dagger\dagger\dagger\dagger}$	L	$(uT\tau+\tau\lambda+\tau pT+p\delta T)L/3$

† In every row of $\mathbf{H}$, which is Φ in this case, only N_{Ch} out of N elements are non-zero.
†† In ψ, only vML complex elements are nonzero.
††† λ refers to number of real multiplications required for *tanh* function.
†††† δ and τ refers to number of real multiplications required for *sigmoid* function and the number of nodes of the hidden layer of FCNN, respectively.

Table 5.2 : Summary of the Computational Complexity of ZF, ML and Deep-SMX-IM Detectors for MIMO-GFDM-IM

Detector	*Total Complexity (CMs)*
ZF	$N^3(T^3+2T^2R)+N^2(RT+N_{CH}RT)+NcQ^vT$
ML	$(cQ^v)^{TN/u}\left((N^2TRv/u)+NT\right)+N_{\mathrm{Ch}}N^2RT$
Deep-SMX-IM	$N_{\mathrm{Ch}}N^2RT+2N^3T^2R+N^3T^3+N^2RT+(2uFT+uT\lambda)ML/3+(uT\tau+\tau\lambda+\tau pT+p\delta T)L/3$

Table 5.3 : The Total Number of CMs for ZF, ML and Deep-SMX-IM Detectors for MIMO-GFDM-IM

Configuration	*ZF*	*Deep-SMX-IM*	*ML*
BPSK $T=2,R=2$	4.53×10^{8}	4.53×10^{8}	3.29×10^{76}
4-QAM $T=2,R=2$	4.53×10^{8}	4.53×10^{8}	3.08×10^{134}
BPSK $T=4,R=4$	2.31×10^{11}	2.31×10^{11}	1.83×10^{178}
4-QAM, $T=4,R=4$	2.31×10^{11}	2.31×10^{11}	1.08×10^{294}

Table 5.4 : Fine Detector Model Summary for SMX-IM

Layer	*Output Shape*	*Activation Func.*
Input	(B,2,u,T)	None
Conv2d	(B,1,u,F)	tanh
Flatten	(B,uF)	None
Dense	(B,τ)	tanh
Dense	(B,pT)	sigmoid

Table 5.5 : Fine Detector Model Parameters for SMX-IM

Antenna Configuration	*Modulation*	*Parameter*	*Value*
2×2	BPSK	F	64
		τ	128
	4-QAM	F	64
		τ	256
4×4	BPSK	F	128
		τ	256
	4-QAM	F	128
		τ	256

6. CONCLUSIONS AND RECOMMENDATIONS

In this thesis, GFDM, GFDM-IM, and SMX-IM receiver schemes have been investigated and deep learning aided novel receiver structures have been introduced for future wireless networks.

In the first stage of the thesis, a novel DL-aided GFDM detection and demodulation scheme, which is constructed by a combination of a linear detector and a neural network, has been proposed. This application would be the first attempt to exploit a neural network for GFDM detection. Besides, MMSE detector is proposed for the coarse detection stage of the cascaded approach. Furthermore, a CNN is exploited to handle complex signals, i.e., QAM signals, through FCNN. BER performance of the proposed scheme has been compared to classical linear detector. It has been demonstrated that the proposed scheme provides significant BER improvement compared to classical linear detectors.

In the second stage of the thesis, a novel deep convolutional neural network-based detector, termed as DeepConvIM, is proposed for GFDM-IM scheme. The proposed scheme is constructed by the combination of a ZF detector and a deep convolutional neural network. This two-stage approach prevents the getting stuck of neural networks in a saddle point and enables IM blocks processing independently. The FCNN part uses only two fully-connected layers, which can be adapted to yield a trade-off between complexity and BER performance. Also, this scheme has a very simple and flexible neural network structure, which can be adapted to yield a trade-off between complexity and BER performance. The proposed method would be the first attempt to exploit a neural network for GFDM-IM detection. Furthermore, a CNN approach is used to detect IM scheme for the first time. BER performance of the proposed scheme has been compared to ZF and ML detectors. It has been demonstrated that the proposed scheme provides significant BER improvement compared to ZF detector with a reasonable complexity increase.

In the third stage of the thesis, a DNN-aided detector is proposed for the combined application of SMX MIMO transmission, GFDM and IM for the purpose of improving error performance without increasing complexity. To use CNN and FCNN provide to learn the transmission characteristics of spatial and frequency multiplexing, respectively. Note that, a CNN approach provides a flexible structure for SMX transmission thanks to supporting multi-channel operation and preserving the spatial dependence. Besides, using IM enables to implement subblock-based detection, which simplifies the DL model and reduces the complexity. The proposed method would be the first appearance to implement DL-aided SMX-IM detection. It has been shown that the proposed method has an important BER gain competed with ZF detector without increasing complexity.

In this thesis, DL aided JDD for GFDM, DeepConvIM for GFDM-IM and Deep-SMX-IM for MIMO-GFDM-IM have been proposed. All models provide significant BER performance but while DL aided JDD has the highest complexity, Deep-SMX-IM has the lowest complexity. The use of index modulation techniques in DL aided detection methods ensures that DL models are of low complexity. Furthermore, the combination of SMX and IM ensures that the complexity remains almost the same compared to the linear detector. The significant advantages of deep learning architectures should be used according to reflecting the characteristics physical layer. It has been concluded that deep learning aided data detection methods are a promising area for the next generation of wireless communication.

REFERENCES

[1] **3GPP** (2017). NR, Physical layer, General description, *tech. spec. 38.201*.

[2] **3GPP** (2017). Study on New Radio (NR) access technologies, *tech. rep. 38.912 V14.1.0*.

[3] **Wunder *et. al.*, G.** (2014). 5GNOW: Non-orthogonal, asynchronous waveforms for future mobile applications, *52*(2), 97–105.

[4] **Michailow, N.**, **Matthe, M.**, **Gaspar, I.**, **Caldevilla, A.**, **Mendes, L.**, **Festag, A. and Fettweis, G.** (2014). Generalized frequency division multiplexing for 5th generation cellular networks, *62*(9), 3045–3061.

[5] **Basar *et. al.*, E.** (2017). Index Modulation Techniques for Next-Generation Wireless Networks, *IEEE Access*, *5*(1), 16693–16746.

[6] **Mesleh, R.**, **Haas, H.**, **Sinanovic, S.**, **Ahn, C.W. and Yun, S.** (2008). Spatial modulation, *57*(4), 2228–2241.

[7] **Di Renzo et. al., M.** (2014). Spatial Modulation for Generalized MIMO: Challenges, Opportunities, and Implementation, *Proceedings of the IEEE*, *102*(1), 56–103.

[8] **Basar, E.**, **Aygölü, Ü.**, **Panayırcı, E. and Poor, H.V.** (2013). Orthogonal frequency division multiplexing with index modulation, *61*(22), 5536–5549.

[9] **Abu-alhiga, R. and Haas, H.** (2009). Subcarrier-index modulation OFDM, *IEEE Int. Sym. Personal, Indoor and Mobile Radio Commun.*, Tokyo, Japan, pp.177–181.

[10] **Tsonev, D.**, **Sinanovic, S. and Haas, H.** (2011). Enhanced subcarrier index modulation (SIM) OFDM, *IEEE GLOBECOM Workshops*, pp.728–732.

[11] **Ozturk, E.**, **Basar, E. and Cirpan, H.** (2016). Spatial Modulation GFDM: A Low Complexity MIMO-GFDM System For 5G Wireless Networks, *Proc. 4th IEEE Int. Black Sea Conf. Commun. Networking*, Varna, Bulgaria.

[12] **Ozturk, E.**, **Basar, E. and Cirpan, H.** (2016). Generalized frequency division multiplexing with index modulation, *Proc. IEEE GLOBECOM Workshops*, Washington DC, USA.

[13] **Ozturk, E.**, **Basar, E. and Cirpan, H.** (2017). Generalized Frequency Division Multiplexing with Space and Frequency Index Modulations, *Proc. 5th IEEE Int. Black Sea Conf. Commun. Networking*, Istanbul, Turkey.

[14] **Ozturk, E.**, **Basar, E. and Cirpan, H.** (2017). Generalized Frequency Division Multiplexing with Flexible Index Modulation, *IEEE Access*, *5*, 24727 – 24746.

[15] **Ozturk, E.**, **Basar, E. and Cirpan, H.** (2018). Generalized Frequency Division Multiplexing with Flexible Index Modulation Numerology, *25*(10), 1480–1484.

[16] **Ozturk, E.**, **Basar, E. and Cirpan, H.** (2019). Multiple-Input Multiple-Output Generalized Frequency Division Multiplexing with Index Modulation Numerology, *Physical Communication*, *34*, 27–37.

[17] **Goodfellow, I.**, **Bengio, Y. and Courville, A.** (2016). *Deep Learning*, MIT Press, `http://www.deeplearningbook.org`.

[18] **You, L.**, **Yang, P.**, **Xiao, Y.**, **Rong, S.**, **Ke, D. and Li, S.** (2017). Blind Detection for Spatial Modulation Systems Based on Clustering, *IEEE Communications Letters*, *21*(11), 2392–2395.

[19] **Soltani, M.**, **Mirzaei, A.**, **Pourahmadi, V. and Sheikhzadeh, H.** (2018). Deep Learning-Based Channel Estimation.

[20] **Huang, Q.**, **Zhao, C.**, **Jiang, M.**, **Li, X. and Liang, J.** (2018). Cascade-Net: a New Deep Learning Architecture for OFDM Detection, *[Online]. Available: arXiv:1812.00023v1, preprint*.

[21] **Zhao, Z.**, **Vuran, M.**, **Guo, F. and Scott, S.** (2018). Deep-Waveform: A Learned OFDM Receiver Based on Deep Complex Convolutional Networks, *arXiv:1810.07181 [eess.SP]*.

[22] **O'Shea, T.J.**, **Karra, K. and Clancy, T.C.** (2016). Learning to communicate: Channel auto-encoders, domain specific regularizers, and attention, *2016 IEEE International Symposium on Signal Processing and Information Technology (ISSPIT)*, pp.223–228.

[23] **Q'Shea, T. and Hoydis, J.** (2017). An Introduction to Deep Learning for the Physical Layer, *IEEE Tran. on Cognitive Comm. and Networking*, *3*(4), 563–574.

[24] **Q'Shea, T.**, **Erpek, T. and Clancy, T.C.** (2017). Deep Learning-Based MIMO Communications, *arXiv:1707.07980*.

[25] **Samuel, N.**, **Diskin, T. and Wiesel, A.** (2017). Deep MIMO detection, *2017 IEEE 18th International Workshop on Signal Processing Advances in Wireless Communications (SPAWC)*, `http://dx.doi.org/10.1109/SPAWC.2017.8227772`.

[26] **Corlay, V.**, **Boutros, J.J.**, **Ciblat, P. and Brunel, L.** (2018). Multilevel MIMO Detection with Deep Learning, *CoRR*, *abs/1812.01571*, `http://arxiv.org/abs/1812.01571`, `1812.01571`.

[27] **He *et. al.*, H.** (2018). A Model-Driven Deep Learning Network for MIMO Detection, *arXiv:1809.09336*.

[28] **Huang, C.**, **Alexandropoulos, G.C.**, **Zappone, A.**, **Yuen, C. and Debbah, M.** (2019). Deep Learning for UL/DL Channel Calibration in Generic Massive MIMO Systems, *CoRR*, `http://arxiv.org/abs/1903.02875`.

[29] **Luong, T.V.**, **Ko, Y.**, **Vien, N.A.**, **Nguyen, D.H.N. and Matthaiou, M.** (2019). Deep Learning-Based Detector for OFDM-IM, *IEEE Wireless Communications Letters*, *8*(4), 1159–1162.

[30] **Turhan, M.**, **Ozturk, E. and Cirpan, H.** (2019). Deep Learning Aided Generalized Frequency Division Multiplexing.

[31] **Turhan, M.**, **Ozturk, E. and Cirpan, H.** (2019). Deep Convolutional Learning-Aided Detector for Generalized Frequency Division Multiplexing with Index Modulation.

[32] **Zhang, C.**, **Patras, P. and Haddadi, H.** (2018). Deep Learning in Mobile and Wireless Networking: A Survey, *IEEE Communications Surveys and Tutorials*, *PP*.

[33] **Mao, Q.**, **Hu, F. and Hao, Q.** (2018). Deep Learning for Intelligent Wireless Networks: Comprehensive Survey, *IEEE Communications Surveys Tutorials*, *20*(4), 2595–2621.

[34] **Wang *et. al.*, T.** (2017). Deep Learning for Wireless Physical Layer: Opportunities and Challenges, *arXiv:1710.05312*.

[35] **Zappone *et. al.*, A.** (2019). Wireless Networks Design in the Era of Deep Learning: Model-Based, AI-Based, or Both?, *arXiv:1902.02647*.

[36] **Bi, S.**, **Zhang, R.**, **Ding, Z. and Cui, S.** (2015). Wireless communications in the era of big data, *IEEE Communications Magazine*, *53*(10), 190–199.

[37] **Kingma, D.P. and Ba, J.**, (2014), Adam: A Method for Stochastic Optimization, `http://arxiv.org/abs/1412.6980`.

[38] **3GPP** (2017). Base Station (BS) radio transmission and reception, *tech. spec. 36.104 V14.4.0*.

[39] **Zeiler, M.D.** (2012). ADADELTA: An Adaptive Learning Rate Method, *CoRR*, *abs/1212.5701*, `http://arxiv.org/abs/1212.5701`.

[40] **Chollet, F.**, **Vura, M.**, **Guo, F. and Scott, S.** (2015). Keras, *https://keras.io*.

[41] **Abadi, M. and et. al** (2015). TensorFlow: Large-scale machine learning on heterogeneous systems, *[Online]. Available: https://www.tensorflow.org/*.

CURRICULUM VITAE

Name Surname: Merve TURHAN

E-Mail: turhanm17@itu.edu.tr

EDUCATION:

- **B.Sc.:** 2016, Istanbul Technical University-Turkish Naval Academy, Electronic and Communication Engineer Department
- **Project Student:** 2019, Telecommunication Circuit Laboratory, École Polytechnique Fédérale de Lausanne, Switzerland.

PROFESSIONAL EXPERIENCE AND REWARDS:

- 2017 - Software Design Engineer, NETAŞ
- 2017 - Master of Science Achievement of Scholarship, TUBITAK
- 2019 - Teaching Assistant, Wireless Receivers: Algorithm and Architecture, École Polytechnique Fédérale de Lausanne, Switzerland

PUBLICATIONS, PRESENTATIONS AND PATENTS ON THE THESIS:

- **Turhan M.**, Ozturk E., Cirpan H. A., 2019. Deep Convolutional Learning-Aided Detector for Generalized Frequency Division Multiplexing with Index Modulation, *IEEE International Symposium on Personal, Indoor and Mobile Radio Communications)*, September 8-11, 2019, Istanbul, Turkey.
- **Turhan M.**, Ozturk E., Cirpan H. A., 2019. Deep Learning-aided Generalized Frequency Division Multiplexing, *(3rd Intl. Balkan Conf. Commun. Networking*, June 10-12, 2019, Skopje, North Macedonia.